This is a preprint, the final version is subject to change, of the American Mineralogist (MSA)
Cite as Authors (Year) Title. American Mineralogist, in press.
(DOI will not work until issue is live.) DOI: http://dx.doi.org/10.2138/am-2015-4939

Revision 1

First Crystal Structure Determination of Alumohydrocalcite and Classification of the Dundasite Group

MARCIN STACHOWICZ[1,2], JAN PARAFINIUK[3], CLAIRE WILSON[4], SIMON COLES[5], KRZYSZTOF WOŹNIAK[2*]

[1]College of Inter-Faculty Individual Studies in Mathematics and Natural Sciences (MISMaP), Żwirki and Wigury 93, 02-089 Warszawa, Poland
[2]Biological and Chemical Research Centre, University of Warsaw, Żwirki i Wigury 101, 02-089 Warszawa, Poland.
[3]Institute of Mineralogy, Geochemistry and Petrology, University of Warsaw, 02-089 Warszawa, Poland.
[4]Diamond Light Source, Harwell Science and Innovation Campus, Didcot, Oxfordshire OX11 0DE, UK.
[5]Faculty of Natural & Environmental Sciences, School of Chemistry, University of Southampton, Highfield, Southampton, SO17 1BJ, UK.

E-mail: kwozniak@chem.uw.edu.pl

ABSTRACT

The crystal structure of alumohydrocalcite was determined using synchrotron X-ray radiation. Alumohydrocalcite crystallizes in the triclinic $P\bar{1}$ space group with unit cell parameters: a = 5.71(5) Å; b= 6.54(4) Å; c=14.6 (2) Å α = 81.8(3)°; β = 83.9(3)°; γ = 86.5(7)° and V = 537(7) Å^3. This mineral has the formula $CaAl_2(CO_3)_2(OH)_4 \cdot 4H_2O$ as opposed to the commonly accepted formula $CaAl_2(CO_3)_2(OH)_4 \cdot 3H_2O$. The fourth water molecule interacts with the strongly-bonded polyhedral unit of the structure through hydrogen bonds and connects three adjacent units. This water molecule plays a major role in crystal stability. On heating the sample, this fourth water molecule escapes from the crystal structure as a first one at lower temperature (*ca.* 128°C) than the other water molecules in the crystal structure (*ca.* 128°C)

Analysis and description of the alumohydrocalcite crystal structure and particularly of the intermolecular interactions, together with a comparison to the

Always consult and cite the final, published document. See http://www.minsocam.org or GeoscienceWorld

crystal structures of other minerals with the analogue formula $M^{2+}M^{3+}{}_2(CO_3)_2(OH)_4 \bullet nH_2O$, suggests that this mineral is an extension of the dundasite group which should, we propose, be formed for all minerals with the above formula. They all exhibit very similar patterns on Hirshfeld surfaces. Hirshfeld surfaces appear to be a very useful tool in the analysis of interactions, classification and validation of mineral crystal structures.

Keywords:
Alumohydrocalcite, hydrate, crystal structure, X-ray diffraction, synchrotron radiation

Introduction

In this work, we use the alumohydrocalcite structural data as a case study to stress the applications of Hirshfeld surfaces as an excellent tool to characterise intermolecular interactions in minerals in general. Hirshfeld surfaces can be computed for all crystal structures determined up to now. We have applied them to alumohydrocalcite, and to a broader group of minerals with already established crystal structures. The potential similarity of the Hirshfeld surface plots can be used as a base for classification of minerals as we have done for the dundasite group demonstrating that alumohydrocalcite forms an extension of this group. In fact, Hirshfeld surfaces can also be used to validate all known mineral structures because incorrect positions of, for example, hydrogen atoms, lead to contradictions in related, so-called, finger print plots.

In this work we also present details of crystal structure of alumohydrocalcite. It was identified by Bilibin (1926) in samples collected near

Always consult and cite the final, published document. See http://www.minsocam.org or GeoscienceWorld

the village of Poliechino, Western Siberia, Russia, and was named by him after the main components of its chemical composition. Although the mineral is known to occur in a few dozen localities around the world, it can still be considered as a rare and not thoroughly investigated species. As it diffracts X-rays very weakly, there have been no published data on the crystal structure of alumohydrocalcite. This mineral begins a series of studies of known minerals with unknown crystal structures.

Alumohydrocalcite has the generally accepted formula: $CaAl_2(CO_3)_2(OH)_4 \cdot 3H_2O$. It usually forms very tiny needle-like crystals, sporadically exceeding 1 mm in length (Figure 1). Because of the poor quality and very small size of the crystals, the crystal structure of alumohydrocalcite has not yet been determined. Crystals of alumohydrocalcite compose small spherules and radial aggregates, but thin, compact encrustations and powdery, earthy masses are also found. Most alumohydrocalcite aggregates are white or pale-coloured, stained by impurities. Chromian varieties are pink to purple. The mineral is very soluble in acids, and is decomposed by boiling water. It crystallizes from low-temperature hydrothermal or carbonated meteoric water acting on argillaceous or carbonate rocks and may be associated with dickite, allophane, gibbsite, calcite, aragonite, siderite, barite, quartz and other minerals.

Figure 1 here

Based on alumohydrocalcite from Nowa Ruda (Lower Silesia, Poland), we propose a crystal structure for this mineral determined by single-crystal X-ray diffraction. Because of the small size of the alumohydrocalcite crystals (for example the size of the measured one was: 70μmx3μmx3μm) and their weak diffraction of X-rays, additionally complicated by multiple integrown, only

Always consult and cite the final, published document. See http://www.minsocam.org or GeoscienceWorld

synchrotron radiation (in this case Diamond, Station I19) permits acceptable quality data collection of the scattered intensities of X-ray radiation good enough to establish this very challenging material.

Occurrence

Nowa Ruda is one of the classic localities for alumohydrocalcite. It was noted by German mineralogists before World War II but erroneously identified as pharmacolite. The correct determination of the species from Nowa Ruda was made by Hoehne (1953). A detailed description of the Nowa Ruda occurrence was published by Morawiecki (1962) who, on the basis of microscopic studies, - classified it wrongly as orthorhombic and as a new species, β-alumohydrocalcite. The new data were disputed (Fleischer, 1963) and the name was rejected by Commission on New Minerals and Mineral Names (IMA, CNMMN, 1967)

Many occurrences of alumohydrocalcite were found in the underground workings of the recently abandoned “Nowa Ruda” colliery and on the nearby mine dump. It occurs in weathered gabbro residues, underlying bituminous coal seams and dark, argillaceous shale which are cut by veins of dickite, kaolinite and calcite. The site is not currently accessible, but specimens from there are preserved in some mineral collections.

Alumohydrocalcite forms small veinlets 1-2 mm thick or thin encrustations covering fractures in the shale. Typical of the Nowa Ruda occurrence are radiating aggregates of fibrous crystals up to 2-3 mm in diameter growing on a calcite matrix (Fig. 1a). Fragile and usually multiply tiny needles of alumohydrocalcite grew on the upper parts of the spheroids (Fig. 1b). Chemical analyses of

Always consult and cite the final, published document. See http://www.minsocam.org or GeoscienceWorld

alumohydrocalcite from Nowa Ruda available in the literature (Table 1) are in very good agreement with the theoretical formula $CaAl_2(CO_3)_2(OH)_4 \bullet 3H_2O$. Beside the white, pure alumohydrocalcite, in Nowa Ruda, a chromian variety also occurs, containing 0.5-3.5% Cr_2O_3 (Hoehne, 1953). It can be distinguished by its pink to dark purple color.

Table 1 here

EXPERIMENTAL METHODS

Thermogravimetric (TG) analysis. 17.652 g of alumohydrocalcite was prepared for thermal analysis. The analysis was carried out on a TA SDT Q600 V20.9 instrument. The ramping temperature was set to 5° C per minute and heating was performed in the range 30°C to 1100° C. Nitrogen flow was set to 30 $ml \cdot min^{-1}$. The second TG analysis was carried out on a TGA Q50 V20.13 Instrument to better determine the water separation stages from the sample. 6.923 g of alumohydrocalcite was heated in the range from 30 to 500°C with 1.5°C step. Nitrogen (30 $ml \cdot min^{-1}$ flow) was used as a balance gas.

X-ray diffraction. Single-crystals of this mineral diffract X-rays very weakly and the high intensity available at the synchrotron was needed to measure data allowing the determination of its crystal structure. A needle-shaped crystal was chosen for data collection, performed at the Diamond Light Source, Station I19. The experiments were carried out at 100K using the cryostream cooling device. Although a simple single-crystal was not located, careful data processing allowed the reciprocal lattice of the major single-crystal component of the chosen needle of the mineral to be indexed. Thus a unique set of reflections could be

Always consult and cite the final, published document. See http://www.minsocam.org or GeoscienceWorld

obtained to allow the structural analysis. The crystal structure was solved by direct methods using the SHELXS-97 program and refined with SHELXL-97.

The refinement was based on F^2 for all reflections except those with negative intensities. Weighted wR factors and all goodness-of-fit S values were based on F^2, whereas conventional R factors were based on the amplitudes, with F set to zero for negative F^2. The $F_o^2 > 2\sigma(F_o^2)$ criterion was applied only for R factor calculations and not to reflections used in the refinement. The R factors based on F^2 are about twice as large as those based on F (Sheldrick, 2008). All hydrogen atoms were located in idealised geometrical positions. Atomic scattering factors were taken from Tables 4.2.6.8 and 6.1.1.4 in the International Crystallographic Tables Vol. C (Wilson, 1992).

RESULTS AND DISCUSSION

Chemical composition - TG studies. Table 1 presents the results of previous chemical analyses of alumohydrocalcite composition (Hoehne, 1953; Morawiecki, 1962). These results showed that the amount of water of crystallisation molecules per formula unit (*pfu*) of alumohydrocalcite is three which is in disagreement with the results obtained from alumohydrocalcites by crystal structure solution and refinement. Due to this discrepancy the chemical analysis was repeated to confirm the new structural information.

To determine the amount of water, the 17.652g of alumohydrocalcite was analysed by thermogravimetric methods. 51% loss of mass was observed up to 823°C. This is caused by alumohydrocalcite decomposition to $2CO_2 + 6H_2O + Al_2O_3 + CaO$, and evaporation of the first two components. The peak around 907°C on the Figure

Always consult and cite the final, published document. See http://www.minsocam.org or GeoscienceWorld

159 2 - reflects $CaCO_3$ decomposition to CO_2 and CaO. The impurity of $CaCO_3$ in the
160 sample was 8.14 wt%.

161 Figur 2 here

162 In the case of four water molecules, the theoretical ratio of the molar masses of
163 CO_2 and H_2O to the molar mass of alumohydrocalcite is equal to 0.554, and 0.530
164 if only three water molecules *pfu* are present. The experimental ratio of H_2O and
165 CO_2 that evaporated during thermal decomposition of alumohydrocalcite in the
166 TG analysis to the mass of the mineral is 0.555. This result is in very good
167 agreement with the presence of four hydrated water molecules *pfu* of
168 alumohydrocalcite.

169 A second TG analysis with smaller 1.5°C/min steps was performed only to
170 identify the separate stages of water loss and to get a more reliable temperature at
171 which the fourth water molecule breaks away from the structure. The process starts
172 (peak growth) at 105°C (see Figure 3) and reaches a maximum at 128°C. This
173 process can be rationalized in such a way that only one of four independent water
174 molecules is interacting by weak H-bonds with other ions (see details in the
175 section on the crystal structure below). The remaining H_2O molecules apparently
176 are bound in a stronger way participating in the first coordination spheres of
177 different cations. As a result the temperature of detachment is higher for the
178 remaining water molecules. The process starts at about 128°C and reaches
179 maximum at 155°C.

180 Figure 3 here

181 To determine if transformation to a structure containing three water molecules in
182 the asymmetric unit, an additional experiment was performed. The crystal, after a
183 first X-ray data collection at 300K, was heated using the Oxford Cryosteam 700+

Always consult and cite the final, published document. See http://www.minsocam.org or GeoscienceWorld

184 device to 378K (105°C) and kept at this temperature for thirty minutes before a
185 second period of data collection at this higher temperature. No diffraction was
186 observed from the sample after this treatment which may indicate that even weak
187 H-bond interactions are important for the stability of the alumohydrocalcite crystal
188 structure. This water molecule may have an important role in linking the larger
189 structural fragments. Its removal appears to destroy the crystallinity of the crystal.
190 Unfortunately, the small amount of the alumohydrocalcite sample prevented
191 further X-ray powder diffraction studies. To recapitulate the correct formula of
192 alumohydrocalcite is $CaAl_2(CO_3)_2(OH)_4 \cdot 4H_2O$ which is confirmed by TG
193 measurements and single-crystal X-ray structural analysis, as we now report
194 below.

195 **Crystal structure of alumohydrocalcite.** Table 2 contains selected
196 crystallographic data and refinement details. The list of atomic coordinates
197 together with equivalent isotropic displacement parameters (*Ueq*) and the
198 components of the tensors of anisotropic displacement parameters (ADPs) are
199 presented in Table 3.

200 Table 2 and Table 3 here

201 All ions in the asymmetric unit of alumohydrocalcite occupy general
202 positions. Displacement ellipsoids and atom labelling scheme are presented in
203 Figure 4. The poor quality of the crystals studied influenced the final quality of the
204 collected data, even using synchrotron.

205 Figure 4 here

206 Both Al(1) and Al(2) cations are octahedrally coordinated by six oxygen
207 atoms (Figure 5). Alternating edge-sharing $Al(1)O_6$ and $Al(2)O_6$ octahedra form
208 chains parallel to the *x*-axis with two Al(1)-Al(2) distances in the chain equal to

Always consult and cite the final, published document. See http://www.minsocam.org or GeoscienceWorld

209 2.83(3) Å and 2.88(3) Å. This chain of Al ions is almost linear with the angle
210 formed by three neighbouring Al cations equal to 178.8(3)^{o}. However, tilting of
211 these octahedra is needed to connect CO_3 groups on either side of a chain of
212 octahedra. This configuration can be illustrated by a pair of angles between planes
213 defined by the closest opposite faces of neighbouring octahedra (Figure 5) which
214 are either equal to 57.6(3)° and 87.5(2)° or 88.9(2)° and 56.3(2)°. The shared
215 edges linking the octahedra are formed by O(7), O(8) and O(9), O(10) hydroxyl
216 oxygen. The remaining O(2), O(3), O(4) and O(5) oxygen atoms in the aluminium
217 first coordination sphere are a part of the carbonate groups [C(1)O(1)O(2)O(3));
218 C(2)O(4)O(5)O(6)]. The Al–O bond lengths vary from 1.88(2) Å for the Al(2)-
219 O(4) bond, to 1.96(2) Å for the Al(2)-O(3) bond.

220 Figure 5 here

221 The asymmetric unit contains one calcium site whose coordination
222 sphere forms tetragonal antiprism created by eight oxygen atoms (Figure 6). Each
223 of the O(1), O(2) and O(3) oxygen atoms building this polyhedron is additionally a
224 part of another C(1) carbonate group. The oxygen O(9) is from a hydroxyl group.
225 The remaining four oxygen atoms (two O(11), O12 and O13) belong to the water
226 molecules.

227 Figure 6 here

228 The C(1) and C(2) carbon atoms form the CO_3^{2-} groups with O(1), O(2),
229 O(3) and O(4), O(5), O(6) oxygen atoms, respectively. The C(1) carbon bridges
230 two AlO_6 octahedra and three CaO_8 polyhedra. The $C(2)O_3$ group links two
231 neighbouring $Al(1)O_6$, $Al(2)O_6$ octahedra (Figure 7). Each CaO_8 polyhedron
232 shares three edges in total, one edge with another CaO_8 polyhedron and two
233 further edges with the $Al(1)O_6$ and $Al(2)O_6$ neighbouring octahedra.

Always consult and cite the final, published document. See http://www.minsocam.org or GeoscienceWorld

Figure 7 here

One can distinguish infinite broad ribbons along the X-axis in the ac plane (Figure 8). Each such ribbon is composed of atoms constituting the asymmetric part of the unit cell together with their reflection through the centre of symmetry. The ribbons repeat in [010] and [001] in a distance of the cell parameter *b* and *c*, respectively. Formally the symmetry of the ribbons can be described as by one of the rod groups: R2 ($p\bar{1}$).

Figure 8 here

The O(14) water oxygen atom is not a part of the first coordination sphere of any cation in the alumohydrocalcite crystal structure. The surroundings of this water molecule are shown on Figure 9. The molecule is found in a void formed between the edges of the three closest ribbons and it interacts as a proton donor in the hydrogen bonds with four oxygen atoms (O(5), O(6) and O(4), O(6)) from the two neighbouring carbonate groups. Both of the carbonate groups belong to the same infinite ribbon. The $O(14)H_2$ molecule is additionally an acceptor of two hydrogen bond interactions. A donors of these H-bonds are the hydroxyl groups from the $Al(1)O_6$ and $Al(2)O_6$ first coordination spheres. Each of these OH^- groups is a part of a different infinite ribbon located next one to another along the [010] direction. These neighbouring ribbons also interact between each other by additional hydrogen bonds formed by the $O(7)H^-$ and $O(8)H^-$ hydroxyl groups acting as hydrogen donors with oxygen atom acceptor O(6) from the carbonate group. The structural details of the hydrogen bonds formed (lengths and angles) are presented in Table 4.

Figure 9 here

Always consult and cite the final, published document. See http://www.minsocam.org or GeoscienceWorld

Table 4 here

Comparison with other crystal structures

The infrared investigation of double carbonate minerals by Farrell (1977) allowed for grouping dundasite ($PbAl_2(CO_3)_2(OH)_4 \cdot H_2O$ (Cocco et al. 1972), dresserite ($BaAl_2(CO_3)_2(OH)_4 \cdot H_2O$ (Jambor et al. 1969) and strontiodresserite ($(Sr,Ca)Al_2(CO_3)_2(OH)_4 \cdot H_2O$ (Jambor 1977b, Whitfield et al. 2010), into one group of isostructural minerals. The studies by Jambor (1977a) and Farrell (1977) proved that hydrodresserite ($BaAl_2(CO_3)_2(OH)_4 \cdot 3H_2O$ is metastable under ambient conditions. On heating, it breaks down to an orthorhombic crystal structure of dresserite. Later studies of petterdite ($PbCr_2(CO_3)_2(OH)_4 \cdot H_2O$, (Birch et al. 2000), a chromian analogue of dundasite, also showed it to be isostructural with these two minerals. The mineral, kochsándorite $CaAl_2(CO_3)_2(OH)_4 \cdot H_2O$ (Sajó and Szakál 2007), also crystallises in the same space group and has similar unit-cell parameters. We propose the inclusion of all these minerals in the dundasite group. Most of these minerals are isostructural while others differ only in the number of water molecules in the formula unit. Despite the fact that some crystallise in the orthorhombic system and others are triclinic with differing atom organisation, there are strong structural reasons behind such a classification of all the above minerals, as summarised in Table 5.

Table 5 here

Similar structural motifs can be distinguished in the crystal lattices of all the minerals. They all have edge-sharing AlO_6 octahedra which form some infinite chains. Additionally, for crystal structures with one or three water molecules, infinite channels are formed that run in the same direction as the AlO_6 octahedra

Always consult and cite the final, published document. See http://www.minsocam.org or GeoscienceWorld

chains and are formed by rings of AlO_6 octahedra. The channels are filled with one or two water molecules interacting with oxygen atoms from the first coordination spheres around Al^{3+} and M^{2+} cations. The number of water molecules in the crystal structure results in different types of connection (corner/edge) between neighbouring AlO_6 octahedra and $M^{2+}O_9$ polyhedra and different crystal packing.

In the case of dundasite (Cocco et al. 1972) and strontiodresserite (Whitfield et al. 2010), which have only one water molecule in the asymmetric unit, each AlO_6 octahedron forming the rings surrounding the water molecule containing channels (Figure 10a) shares an edge with one $M^{2+}O_9$ polyhedron and one corner with the next polyhedron. For these two minerals, the unit cell parameters are similar and they crystallise in the same orthorhombic *Pnma* space group. The crystal structures for kochsándorite, petterdite and dresserite have not been determined yet although their space group and unit cell parameters from powder diffraction show them to be orthorhombic and all orthorhombic specimens from the group to be isostructural.

Figure 10 here

Hydrodresserite (Szymanski 1982) crystallises with three water molecules in the asymmetric unit. Intermolecular interactions including two additional water molecules decrease the symmetry from the orthorhombic to the triclinic, $P\bar{1}$ space group. Additionally, the connections inside the ring presented in Figure 10b differ from the previous cases. In this case each AlO_6 octahedron shares only one corner with each of the two closest coordination figures around the Ba^{2+} cation unlike sharing a corner with one and an edge with the second BaO_9 polyhedron. This increases the space inside the channels, allowing both water molecules to be accommodated. The third water molecule forms part of the Ba^{2+} coordination

Always consult and cite the final, published document. See http://www.minsocam.org or GeoscienceWorld

sphere replacing one oxygen atom from the Ba^{2+} coordination sphere after the reorganisation of AlO_6 octahedra necessary to increase the volume of the channel (see Figure 11). The crystal structure of alumohydrocalcite with the addition of one new water molecule to the asymmetric unit is different again. This water molecule lies in the position where the AlO_6 octahedron in hydrodresserite was located. This forces a shift of the AlO_6 octahedra in the alumohydrocalcite crystal structure and a loss of connectivity with the $Ca^{2+}O_8$ polyhedra (breaking of the channels shown on Figure 10 for previously mentioned crystal structures of minerals).

Figure 11 here

A hypothetical path showing the reorganisation caused by the increase of the number of the crystallisation water molecules in the crystal structure is presented in Figure 11. Three steps are shown: the first (Figure 11a) is strontiodresserite with only one hydrated water molecule. Addition of two more water molecules would lead to the crystal structure of hydrodresserite (Figure 11b). The water molecule that was already in the crystal structures gets closer to M^{2+} and locates in its coordination sphere. The AlO_6 octahedron that shared an edge with the $M^{2+}O_9$ polyhedron shifts and breaks one of the bonds to enlarge a free space for the water molecule in the first coordination sphere. This increases the volume of the channel shown on Figure 10b. The addition of the fourth water molecule in alumohydrocalcite breaks the ring consisting of polyhedra surrounding hydrated H_2O molecules (Figure 11c). Water molecules get between the AlO_6 octahedra which are pushed away from the $M^{2+}O_9$ polyhedra thus breaking the ring. Two water molecules substitute for the loss of oxygen atoms from the AlO_6

Always consult and cite the final, published document. See http://www.minsocam.org or GeoscienceWorld

331 octahedra in the $M^{2+}O_9$ first coordination sphere. In consequence, the number of
332 oxygen atoms forming the coordination sphere of M^{2+} atom decreases to 8.
333 There is also a similar mineral which contains 6 water molecules *pfu*. It is called
334 para-alumohydrocalcite, $CaAl_2(CO_3)_2(OH)_4 \cdot 6H_2O$, (Srebrodolskii 1977).
335 However, it is not classified as a member of the group because its structure
336 remains unknown.
337 Additional arguments supporting our grouping of minerals into the
338 dundasite group come from analysis of Hirshfeld surfaces (Figure 12), which we
339 now consider.
340 Figure 12 here
341 **Hirshfeld surfaces.** The interactions involving hydrogen atoms can be represented
342 using so-called Hirshfeld surfaces **(**McKinnon et al. 2007) (see Figure 12). We
343 used fingerprint plots generated from Hirshfeld surfaces (Spackman et al. 2002;
344 Spackman and Jayatilaka 2009) to compare interactions between neighbouring
345 molecules. The following weighting function is used to define a Hirshfeld surface:

346
$$w_A(\mathbf{r}) = \frac{\sum_{i \in \text{molecule } A} \rho_i(\mathbf{r} - \mathbf{r}_i)}{\sum_{i \in \text{crystal}} \rho_k(\mathbf{r} - \mathbf{r}_k)},$$

347 where ρ_i is the spherically averaged electron density of the *i*-th atom in the
348 molecule (centred at point $\mathbf{r}_i$) and ρ_k the electron density of *k*-th atom surrounding a
349 particular molecule in the crystal. The Hirshfeld surface for molecule *A* is defined
350 where $w_A(\mathbf{r}) = 0.5$ for every point $\mathbf{r}$ at the surface. Within a Hirshfeld surface, the
351 promolecule electron density (the sum of spherical independent atom model
352 densities) dominates over the procrystal electron density. A variety of properties
353 can be mapped onto Hirshfeld surfaces: properties related to the shape of the

Always consult and cite the final, published document. See http://www.minsocam.org or GeoscienceWorld

surface (e.g. curvature) and also those connected with distances: the external distance from the Hirshfeld surface to an atom belonging to the closest molecules outside the surface (d_e), the internal distance from the surface to an atom inside the surface (d_i) and d_{norm}, which combines both d_e and d_i, each normalised by the van der Waals (vdW) radius for the particular atoms involved in close proximity to the surface.

In contrast to conventional tables containing only the strongest interactions (as for example Table 4), Hirshfeld surfaces permit an analysis of the whole distribution of contacts. In fact one can even estimate the contribution of particular types of intermolecular interactions. In the case of alumohydrocalcite most of them (52%) are contacts between oxygen and hydrogen atoms forming stronger and weaker H-bonds (see Table 6).

Table 6 here

Another useful tool are the so-called "fingerprint plots" of Hirshfeld surfaces (Figure 13). These plots are two-dimensional charts presenting distances (d_i) from atoms located inside the Hirshfeld surface to this surface versus distances from the surface to the atoms from the outside (d_e) of it. All atoms from the asymmetric part of the unit cell were located inside the calculated Hirshfeld surface for preparation of this chart. Fingerprint plots are a helpful tool in recognising and showing similarities in atomic interactions between the members of a proposed group of related minerals. The fingerprint plots for strontiodresserite and hydrodresserite were calculated in the same way as that for alumohydrocalcite presented on Figure 16. Such plots should supply reasonable values for d_e and d_i distances. When these distances approach zero, this means that the position of some atoms participating in the analysed interactions are not correct. This is the

Always consult and cite the final, published document. See http://www.minsocam.org or GeoscienceWorld

379 case for strontiodresserite and hydrodresserite. There is OH…O hydrogen bonding
380 in these crystal structures and apparently some positions of H-atoms are not
381 correct. The distances of these atoms converge to the Hirschfeld surface (to 0 on
382 the fingerprint plot) for these crystal structures, which is a clear evidence that
383 positions of hydrogen atoms are wrong.

384 Figure 13 here

385 All the most significant interactions found for alumohydrocalcite and
386 illustrated in Figure 16 (OH…O; Al…O; M^{2+}…O, H…H, O…O, C…O), can also
387 be identified for the other crystal structures (Figure13). The visual similarity of all
388 plots for the dundasite group is very convincing and is our base for their joint
389 classification. The contributions of interatomic contacts within each crystal
390 structure type represented by strontiodresserite, hydrodresserite and
391 alumohydrocalcite are presented in Table 6.

392 **CONCLUSIONS**

393 The crystal structure of alumohydrocalcite has been established by
394 synchrotron X-ray radiation. The formula differs from that previously known by
395 one additional water molecule. The results of thermal analysis of
396 alumohydrocalcite clearly confirm this finding. The correct formula of
397 alumohydrocalcite is $CaAl_2(CO_3)_2(OH)_4 \cdot 4H_2O$.

398 On the basis of the structural similarity of the crystal motifs, we propose to
399 extend the dundasite group of minerals to include dundasite, dresserite,
400 strontiodresserite, petterdite, kochsándorite, hydrodresserite and
401 alumohydrocalcite. For all these minerals with established crystal structures,
402 similar Al-M^{2+}-M^{2+}-Al polyhedra and similar interactions can be found. In the case
403 of minerals with as yet undetermined crystal structures, powder diffraction and IR

Always consult and cite the final, published document. See http://www.minsocam.org or GeoscienceWorld

404 spectroscopy experiments suggests that they are likely to be isostructural with
405 those mentioned above with already known topologies. The differences in the
406 intermolecular interactions can be related to the position and number of water
407 molecules. In dundasite, strontiodresserite (one water molecule of crystallisation)
408 and hydrodresserite (three water molecules) some infinite channels surrounding
409 H_2O molecules are created in the crystal lattices. In the case of alumohydrocalcite,
410 a presence of the fourth H_2O molecule breaks the polyhedral rings of the
411 previously mentioned infinite channels.

412 Hirshfeld surfaces and fingerprint plots appear to be very useful tools in
413 representing H-bond and other weak interactions in minerals. The characteristic
414 patterns obtained on fingerprint plots for different minerals of the dundasite group
415 confirm the proposed classification which has been obtained as a result of a
416 detailed structural analysis focused on relationship between packing of
417 coordination polyhedra of cations and their interactions with water moieties.

418

419 **IMPLICATIONS**

420 This work stresses the role of Hirshfeld surfaces and their possible
421 applications in mineralogy. They can be used to characterise
422 interatomic/intermolecular interactions. Characteristic patterns on fingerprint plots
423 and Hirshfeld surfaces form a solid base for the detection of similarity of minerals.
424 Thus they can be used in mineral classification, within or between, different
425 groups. Hirshfeld surfaces are also an excellent tool for the validation of
426 previously determined crystal structures. In general, Hirshfeld surfaces are a
427 universal tool for the analysis and clarification of interactions in minerals.

Always consult and cite the final, published document. See http://www.minsocam.org or GeoscienceWorld

Additionally, this paper brings the first detailed determination of alumohydrocalcite crystal structure based on a single-crystal study using synchrotron X-ray radiation. Our study confirms that crystals even as small as a few μm in size and multiply intergrown, can be structurally analysed when synchrotron radiation is used. The structural data have filled a rather confusing gap in our knowledge of this quite common phase, known since1926. According to the results of our structural and chemical studies, a revision of the chemical formula of alumohydrocalcite is necessary.

ACKNOWLEDGMENTS

The research for this paper was in part supported by the EU through the European Social Fund, contract number UDA-POKL.04.01.01-00-072/09-00. KW thanks for financial support within the Polish National Science Centre grant - decision DEC-2011/03/B/ST10/05491. The study was carried out at the Biological and Chemical Research Centre, University of Warsaw, established within the project co-financed by European Union from the European Regional Development Fund under the Operational Programme Innovative Economy, 2007 – 2013

REFERENCES CITED

Bilibin, G.A. (1926) Alumohydrocalcite – a new mineral. Zapiski Rossiyskogo Mineralogicheskogo Obshchestva, 55, (4), 243-258 (in Russian), abstracted in: American Mineralogist (1928), 13, 569.

Always consult and cite the final, published document. See http://www.minsocam.org or GeoscienceWorld

Birch, W.D., Kolitsch, U., Witzke, T., Nasdala, L., and Bottrill, R.S. (2000) Petterdite, the Cr-dominant analogue of dundasite, a new mineral species from Dundas, Tasmania, Australia and Callenberg, Saxony, Germany. Canadian Mineralogist, 38, 1467-1476.

Cocco, G., Fansani, L., Nunzi, A., and Zanazzi, P.F. (1972) The crystal structure of dundasite. Mineralogical Magazine, 38, 564-569.

Fleischer, M. (1963) New Mineral Names. American Mineralogist, 48, 212.

Hoehne, K. (1953) Ein neues Vorkommen von chromhaltigem Alumohydrocalcit im niederschlesischen Bergbaugebiet. Neues Jahrbuch für Mineralogie Monatshefte, 45-50 (in German).

International Mineralogical Association: Commission on New Minerals and Mineral Names (1967), 36, 133.

Jambor, J.L., Fong, D.G., and Sabina, A.P. (1969) Dresserite, a new barium analogue of dundasite. Canadian Mineralogist, 10, 84-89.

Jambor, J.L., Sabina, A.P., and Sturman, B.D. (1977a) Hydrodresserite, a new Ba-Al carbonate from a silicocarbonatite sill, Montreal Island, Quebec. Canadian Mineralogist, 15, 399-404.

Jambor, J.L., Sabina, A.P., and Sturman, B.D. (1977b) Strontiodresserite, a new Sr-Al carbonate from Montreal Island, Quebec. Canadian Mineralogist, 15, 405-407.

McKinnon, J.J., Jayatilaka, D., and Spackman, M.A. (2007) Towards quantitative analysis of intermolecular interactions with Hirshfeld surfaces. Chemical Communications, 37, 3814 – 3816.

Morawiecki, A. (1962) β-alumohydrocalcite from Nowa Ruda. Kwartalnik Geologiczny, 6 (4), 539-573 (in Polish).

Always consult and cite the final, published document. See http://www.minsocam.org or GeoscienceWorld

476 Sajó, I.E., and Szakál, S. (2007) Kochsándorite, a New Ca-Al carbonate mineral
477 species from the Mány coal deposit, Hungary. Canadian Mineralogist, 45, 479-
478 483.
479 Sheldrick, G.M. (2008) A short history of SHELX. Acta Crystallographica, A64,
480 112–122.
481 Spackman, M.A., and Jayatilaka, D. (2009) Hirshfeld surface analysis.
482 CrystEngComm, 11, 19-32.
483 Spackman, M.A., and McKinnon, J.J. (2002) Fingerprinting Intermolecular
484 Interactions in Molecular Crystals. CrystEngComm, 4, 378-392.
485 Srebrodolskii, V.I. (1977) Para-alumohydrocalcite, a new mineral. Zapiski
486 Rossiyskogo Mineralogicheskogo Obshchestva, 106, 336-337 (in Russian).
487 Szymanski, J.T. (1982) The crystal structure of hydrodresserite, $BaAl_2(CO_3)(OH)_4$
488 $3H_2O$. The Canadian Mineralogist, 20, 253–262.
489 Whitfield, P.S., Mitchell, L.D., Le Page, Y., Margeson, J., and Roberts, A.C.
490 (2010) Crystal structure of the mineral strontiodresserite from laboratory. Powder
491 Diffraction Journal, 25, 322-328.
492 Wilson, A.J.C., Ed., (1992) International Tables for Crystallography, Volume C.
493 Kluwer, Dordrecht.
494
495 **Figure 1.** (a) Radial aggregates of alumohydrocalcite from Nowa Ruda (SEM), (b)
496 morphology of alumohydrocalcite crystals (SEM).
497
498 **Figure 2**. Thermal analysis of alumohydrocalcite with 5°C/min heating.
499

Always consult and cite the final, published document. See http://www.minsocam.org or GeoscienceWorld

Figure 3. Water loss from alumohydrocalcite (the TGA mass measurement with 1.5°C/min step).

Figure4. Thermal ellipsoids at the 50% probability level for alumohydrocalcite.

Figure 5. The first coordination spheres of the aluminium cations. Each octahedron shares one edge with two neighbouring Al- octahedra. The Al(1)–Al(2) distances in the chain are: 2.83(3) Å and 2.88(3) Å. The angles between the closest opposite faces of octahedra are shown as red and blue planes on the left side of the figure. Analogous angles are given on the right side.

Figure 6. The $CaO_3(OH)(H_2O)_4$ tetragonal antiprism of alumohydrocalcite.

Figure 7. The strongly-bonded polyhedral aggregate of alumohydrocalcite centred on a centre of symmetry.

Figure 8. An infinite ribbon of ions and water molecules – projection along the *a*-axis.

Figure 9. The local environment of the O(14) water molecule showing its association with three adjacent polyhedral units with which it forms hydrogen bonds. Broken lines represent hydrogen bonds. H-bonds in which O(14) is involved are marked by magenta colour lines. H-bonds in turquoise colour are also binding neighbouring ribbons independently from O(14) water molecules.

Always consult and cite the final, published document. See http://www.minsocam.org or GeoscienceWorld

525 **Figure 10**. The strongly-bonded unit common of the dundasite group of minerals
526 consisting of Al – M^{2+} – M^{2+} – Al polyhedra. (a) dundasite and strontiodresserite –
527 ; (b) hydrodresserite; (c) alumohydrocalcite

528

529 **Figure 11**. The surroundings of the M^{2+} site and their modification related to the
530 number of water molecules. (a) Sr/Ca atom site environment in strintiochevkinite;
531 (b) Ba^{2+} atom environment in dresserite; (c) Ca^{2+} atom environment in
532 alumohydrocalcite. The light blue plane shows the Al – M^{2+} – M^{2+} – Al
533 coordination spheres interactions present in all structures from the group. Green
534 arrows point where additional water would locate and red arrows show how
535 particular octahedra would reorganise to obtain the packing of the next, more
536 hydrated mineral. Green dashed lines show the path of bond formation in next
537 structure.

538

539 **Figure 12**. Projestion of the Hirshfeld surface (McKinnon, et al. 2007) around
540 assymetric unit of (a) strontiodresserite; (b) hydrodresserite; (c)
541 alumohydrocalcite. The colour scale on the surface represents the shortest
542 distances from the surface coordinate to the closest atom outside or inside the
543 surface. Red corresponds to the shortest contacts(-0.90(5) Å), blue to the longest
544 (1.05(4) Å).

545

546 **Figure 13.** Comparison of fingerprint plots for the members with known crystal
547 structure of the dundasite group of minerals. Because dundasite does not have
548 hydrogen atoms found in its crystal structure, it was not taken for this comparison.

549

550

Always consult and cite the final, published document. See http://www.minsocam.org or GeoscienceWorld

551 **Table 1.** Chemical composition of alumohydrocalcite from Nowa Ruda.

	1	2	3	4	5
Al_2O_3	30.33	28.87	26.97	27.09	28.79
FeO	-	0.16	0.28	-	-
Cr_2O_3	-	0.37	0.28	1.10	-
CaO	16.68	17.42	16.43	14.41	15.83
CO_2	26.19	26.28	23.71	45.60	24.85
H_2O	26.80	25.78	23.48		30.52
Insoluble fraction	-	1.2	8.91	11.81	-
Total	**100**	100.08	100.06	100.01	**100**

552 **1. $CaAl_2(CO_3)_2(OH)_4 \cdot 3H_2O$; 2. Nowa Ruda, average of 3 analysis**
553 **(Morawiecki, 1962); 3. Nowa Ruda (Morawiecki, 1962); 4. Chromian**
554 **variety, Nowa Ruda (Hoehne, 1953); 5. $CaAl_2(CO_3)_2(OH)_4 \cdot 4H_2O$**
555
556
557 **Table 2.** Crystal data and structure refinement details for alumohydrocalcite.

Empirical formula	$C_2H_{12}Al_2CaO_{14}$
Formula weight	344.08
Temperature/K	100(2)
Crystal system	triclinic
Space group	$P\bar{1}$
a/Å	5.71(5)
b/Å	6.54(4)
c/Å	14.6 (2)
α/°	81.8(3)
β/°	83.9(3)
γ/°	86.5(7)
V/Å^3	537(7)

Z	2
ρ_{calc}/mg/mm^3	2.19
μ/mm^{-1}	0.83
F(000)	364.0
Crystal dimensions (mm)	0.07 x 0.003 x 0.003
Radiation wavelength (Å)	0.6889
2Θ range for data collection	2.82 to 52.49°
Index ranges	$-7 \leq h \leq 7$, $-8 \leq k \leq 8$, $-18 \leq l \leq 18$
Reflections collected	6997
Independent reflections	6997[R(int) =0.102]
Data/restraints/parameters	6997/44/210
Goodness-of-fit on F^2	1.016
Final R indices [I>=2σ (I)]	R1 = 0.1097, wR2 = 0.2871
Final R indice [all data]	R1 = 0.1545, wR2 = 0.3303
Largest diff. peak/hole / eÅ^{-3}	2.84/-1.47

558

559 **Table 3.** Fractional atom coordinates and equivalent Anisotropic Displacement Parameters (Å^2) for alhydrocalcite. U_{eq} is defined as 1/3 of the trace of

560 the orthogonalised U^{IJ} tensor. The Anisotropic Displacement Parameter exponent takes the form: $-2\pi^2[h^2a^{*2}U^{11}+...+2hka\times b\times U^{12}]$.

	x	***y***	***z***	U_{eq}	U^{11}	U^{22}	U^{33}	U^{23}	U^{13}	U^{12}
Ca	0.3112(4)	1.1032(4)	0.6052(2)	0.0157(7)	0.015(2)	0.015(2)	0.016(2)	-0.0001(9)	-0.0021(9)	0.0011(9)
Al(1)	0.4484(5)	1.1974(5)	0.2018(2)	0.0091(8)	0.006(2)	0.010()	0.0110(2)	-0.001(2)	-0.001(2)	0.0000(1)
Al(2)	-0.0470(5)	1.2003(5)	0.2001(2)	0.0084(8)	0.006(2)	0.008(2)	0.010(2)	-0.000(2)	-0.000(2)	-0.0002(1)
O(1)	0.131(2)	1.202(2)	0.4647(5)	0.018(2)	0.015(4)	0.021(4)	0.017(4)	0.001(3)	0.001(3)	-0.003(3)
O(2)	0.371(2)	1.150(2)	0.3359(5)	0.010(2)	0.007(4)	0.011(4)	0.012(3)	-0.001(3)	-0.003(3)	0.003(3)
O(3)	-0.026(2)	1.159(2)	0.3344(5)	0.012(2)	0.010(4)	0.011(4)	0.015(4)	0.001(3)	-0.005(3)	-0.002(3)
O(4)	0.932(2)	1.231(2)	0.0716(5)	0.014(2)	0.012(4)	0.018(4)	0.011(4)	-0.002(3)	-0.003(3)	0.002(3)
O(5)	0.530(2)	1.228(2)	0.0722(5)	0.013(2)	0.007(4)	0.018(4)	0.013(4)	0.001(3)	-0.001(3)	-0.001(3)
O(6)	0.759(2)	1.263(2)	-0.0612(5)	0.017(2)	0.018(4)	0.014(4)	0.018(4)	-0.004(3)	0.000(3)	0.001(3)
O(7)	0.191(2)	1.393(2)	0.1936(5)	0.008(2)	0.005(4)	0.006(4)	0.013(3)	0.003(3)	-0.001(3)	0.001(3)
O(8)	0.216(2)	1.006(2)	0.1913(5)	0.009(2)	0.008(3)	0.009(3)	0.010(3)	-0.002(2)	-0.001(2)	0.000(2)
O9	0.291(2)	0.997(2)	0.7759(5)	0.010(2)	0.007(4)	0.004(4)	0.018(4)	-0.001(3)	0.000(3)	-0.001(3)
O10	0.685(2)	1.384(2)	0.2174(5)	0.010(2)	0.009(3)	0.010(3)	0.011(3)	0.000(2)	-0.002(2)	0.001(2)

	x	y	z	U_{eq}	U^{11}	U^{22}	U^{33}	U^{23}	U^{13}	U^{12}
O11	0.356(2)	0.803(2)	0.5075(6)	0.016(2)	0.012(4)	0.017(4)	0.018(4)	0.001(3)	-0.001(3)	-0.002(3)
O12	0.449(2)	1.433(2)	0.6306(6)	0.020(2)	0.022(5)	0.016(4)	0.020(4)	-0.006(3)	0.007(4)	0.001(4)
O13	-0.064(2)	1.298(2)	0.6712(6)	0.021(2)	0.018(5)	0.019(5)	0.025(4)	0.002(4)	-0.002(4)	-0.007(4)
O14	0.728(20)	0.732(2)	0.0965(5)	0.015(2)	0.011(4)	0.019(4)	0.016(4)	-0.001(3)	0.001(3)	-0.003(3)
C1	0.161(2)	1.170(2)	0.3794(7)	0.009(2)	0.008(3)	0.008(3)	0.011(3)	0.000(3)	0.000(3)	-0.003(3)
C2	0.740(2)	1.244(2)	0.0271(7)	0.010(2)	0.007(6)	0.012(5)	0.011(5)	-0.001(4)	-0.002(4)	-0.002(4)

561 **Table 4.** Hydrogen bonds (Å, °) in the alumohydrocalcite structure.

D	H	A	*d*(D-H)	*d*(H-A)	*d*(D-A)	∠ D-H-A
O7	H7	O6[h]	0.92(8)	1.86(9)	2.76(2)	164(11)
O8	H8	O6[a]	0.81(8)	2.0(1)	2.76(2)	155(14)
O9	H9	O14[d]	0.86(7)	1.91(8)	2.74(2)	161(13)
O10	H10	O14[i]	0.89(8)	1.80(8)	2.68(2)	169(11)
O11	H11A	O1[b]	0.89(6)	1.93(8)	2.77(3)	157(12)
O11	H11B	O12[c]	0.89(6)	2.01(7)	2.86(2)	160(11)
O12	H12A	O10[e]	0.85(7)	1.92(7)	2.70(2)	152(10)
O12	H12B	O13[f]	0.91(7)	2.2(2)	2.96(3)	141(12)
O13	H13B	O8[b]	0.96(8)	2.0(2)	2.73(2)	131(12)
O14	H14A	O5[a]	0.91(8)	2.11(7)	2.98(2)	160(10)
O14	H14B	O4[g]	0.93(7)	2.23(9)	2.96(2)	135(7)
O14	H14B	O6[g]	0.93(7)	2.03(7)	2.92(3)	160(10)

562 [a]1-X,2-Y,-Z; [b]-X,2-Y,1-Z; [c]+X,-1+Y,+Z; [d]1-X,2-Y,1-Z; [e]1-X,3-Y,1-Z; [f]1+X,+Y,+Z; [g]2-X,2-Y,-Z; [h]1-X,3-Y,-Z; [i]+X,1+Y,+Z

563

564 **Table 5**. Dundasite group of minerals.

Mineral name	**Formula**	**Space group**	***a* [Å]**	***b* [Å]**	***c* [Å]**
dundasite	$PbAl_2(CO_3)_2(OH)_4 \cdot H_2O$	*Pnma*	16.321(9)	5.786(7)	9.079(3)
dresserite	$BaAl_2(CO_3)_2(OH)_4 \cdot H_2O$	*Pnma*	16.83	5.63	9.27
strontiodresserite	$(Sr,Ca)Al_2(CO_3)_2(OH)_4 \cdot H_2O$	*Pnma*	16.0990(7)	5.6133(3)	9.1804(4)
petterdite	$BaCr_2(CO_3)_2(OH)_4 \cdot H_2O$	*Pnma*	16.321(9)	5.786(7)	9.079(3)
kochsándorite	$CaAl_2(CO_3)_2(OH)_4 \cdot H_2O$	*Pnma*	15.564(6)	5.591(4)	9.112(4)
hydrodresserite	$BaAl_2(CO_3)_2(OH)_4 \cdot 3H_2O$	$P\bar{1}$	9.7545(5)	10.4069(5)	5.6322(3)

alumohydrocalcite	$CaAl_2(CO_3)_2(OH)_4{\cdot}4H_2O$	5.71(5)	6.54(4)	14.64(11)

565

566

567

568 **Table 6**. The percentage contribution of interatomic contacts in strontiodresserite,
569 hydrodresserite and alumohydrocalcite.

	Strontiodresserite	**Hydrodresserite**	**Alumohydrocalcite**
O···H	38	34	55
H···H	13	17	21
Al···O	7	26	9
Ca···O	-	-	7
Sr···O	16	-	-
Ba···O	-	11	-
O···O	7	6	5
H···C	3	1	2
Al···H	0	2	1
Ca···H	-	-	0
Sr···H	1	-	-
Ba···H	-	1	-
O···C	15	1	0

570

571

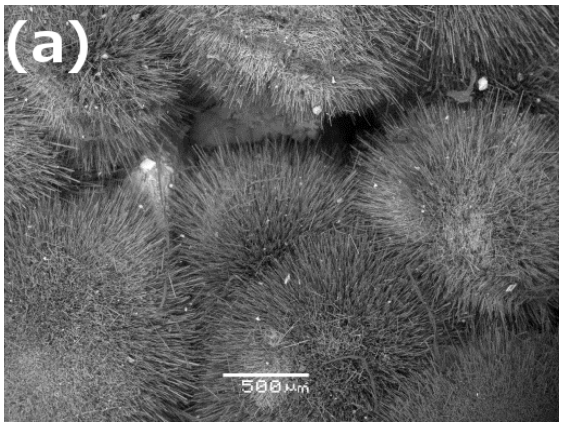

572

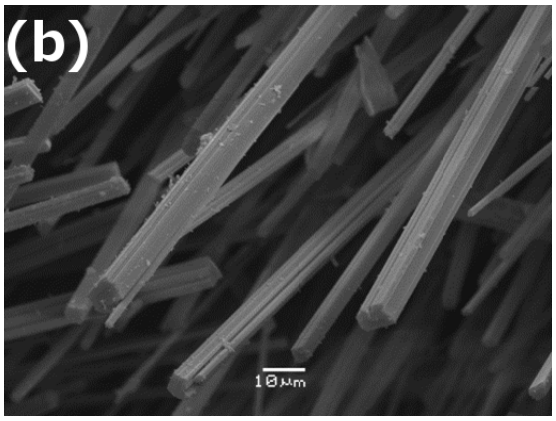

Figure 1. (a) Radial aggregates of alumohydrocalcite from Nowa Ruda (SEM), (b) morphology of alumohydrocalcite crystals (SEM).

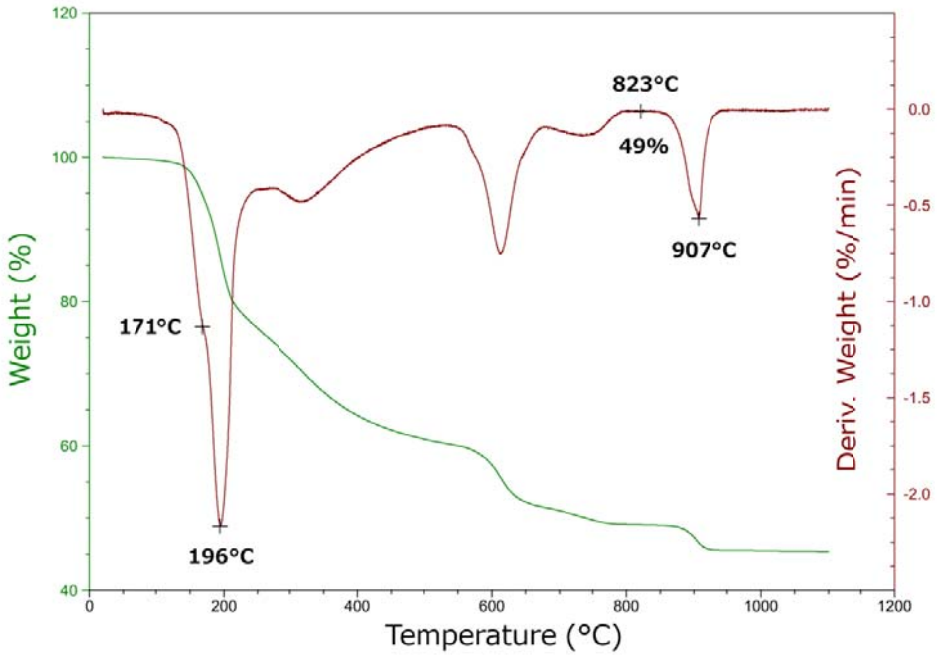

Figure 2. Thermal analysis of alumohydrocalcite with 5°C/min heating.

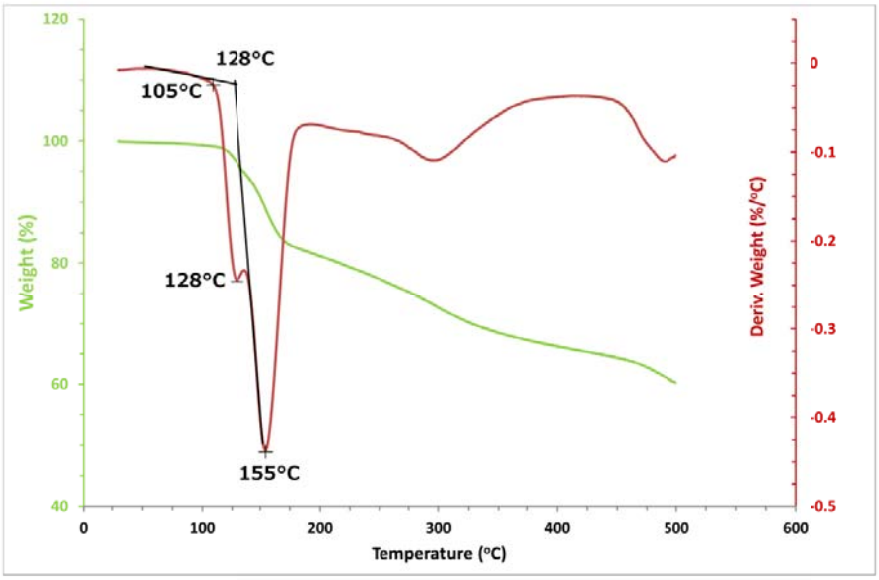

580

581 **Figure 3.** Water loss from alumohydrocalcite (the TGA mass measurement with

582 1.5°C/min step).

583

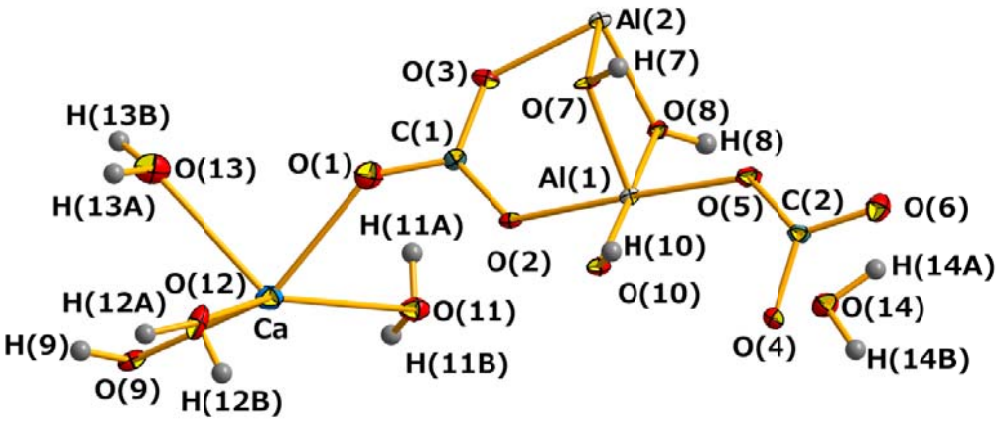

584

585 **Figure 4.** Thermal ellipsoids at the 50% probability level for alumohydrocalcite.

586

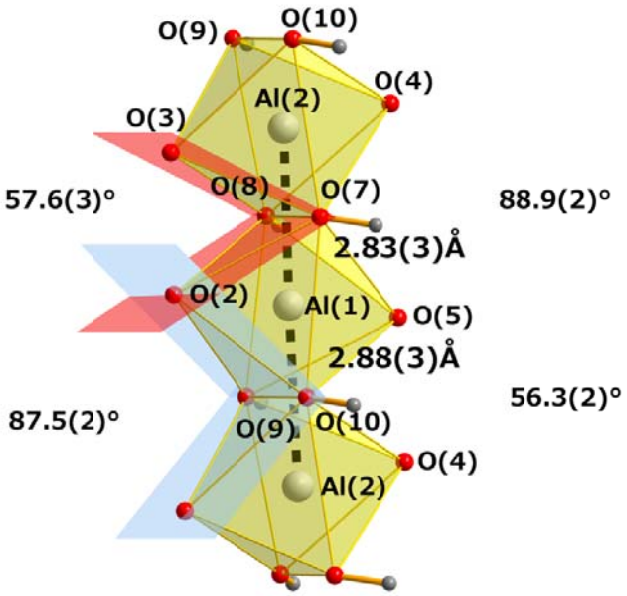

587

588 **Figure 5.** The first coordination spheres of the aluminium cations. Each
589 octahedron shares one edge with two neighbouring Al- octahedra. The Al(1)–Al(2)
590 distances in the chain are: 2.83(3) Å and 2.88(3) Å. The angles between the closest
591 opposite faces of octahedra are shown as red and blue planes on the left side of the
592 figure. Analogous angles are given on the right side.

593

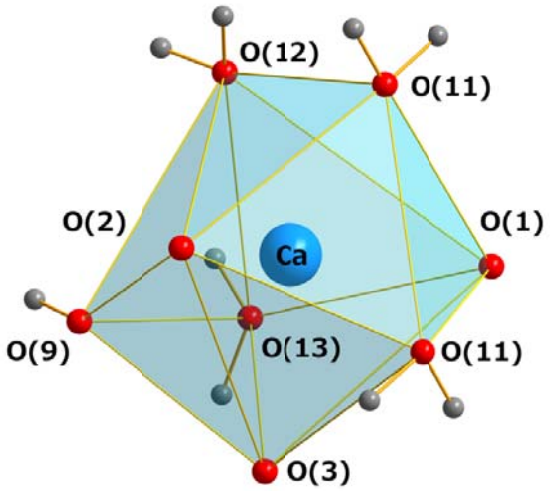

Figure 6. The $CaO_3(OH)(H_2O)_4$ tetragonal antiprism of alumohydrocalcite

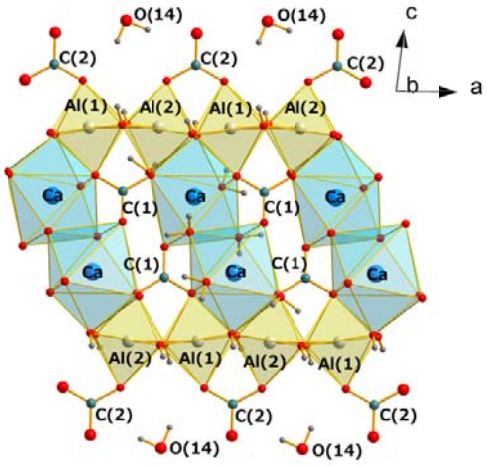

Figure 7. The strongly-bonded polyhedral aggregate of alumohydrocalcite centred on a centre of symmetry.

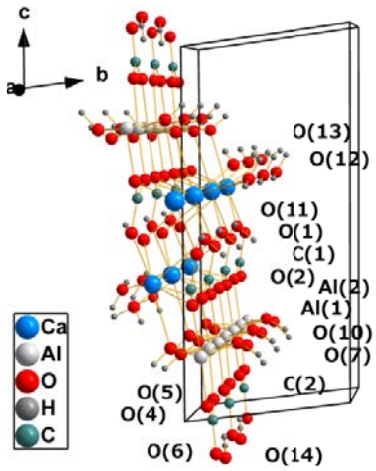

601

602 **Figure 8**. An infinite ribbon of ions and water molecules – projection along the *a*-

603 axis.

604

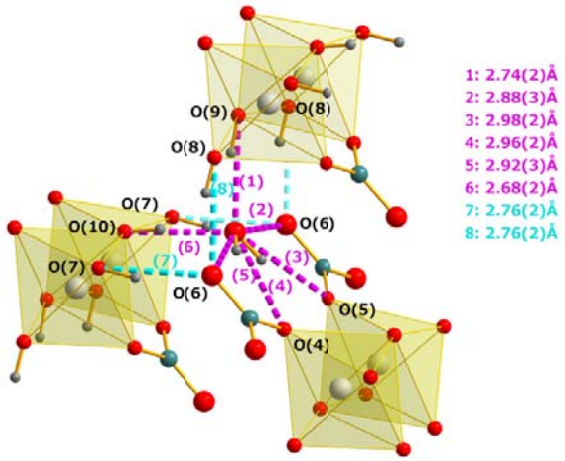

605

606 **Figure 9**. The local environment of the O(14) water molecule showing its

607 association with three adjacent polyhedral units with which it forms hydrogen

608 bonds. Broken lines represent hydrogen bonds. H-bonds in which O(14) is

609 involved are marked by magenta colour lines. H-bonds in turquoise colour are also

610 binding neighbouring ribbons independently from O(14) water molecules.

611

612

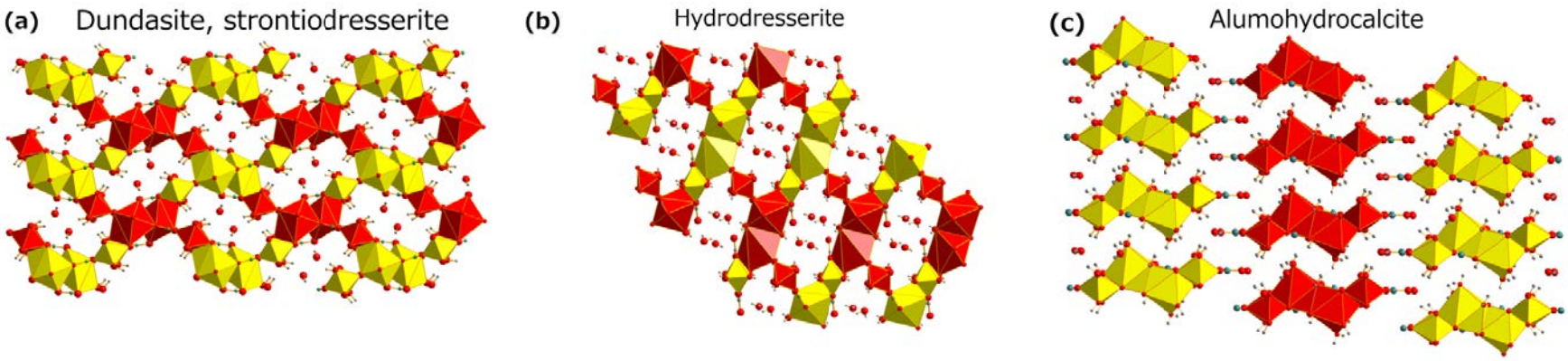

613 **Figure 10**. The strongly-bonded unit common of the dundasite group of minerals consisting of Al – M^{2+} – M^{2+} – Al polyhedra. (a) dundasite and

614 strontiodresserite –; (b) hydrodresserite; (c) alumohydrocalcite

615

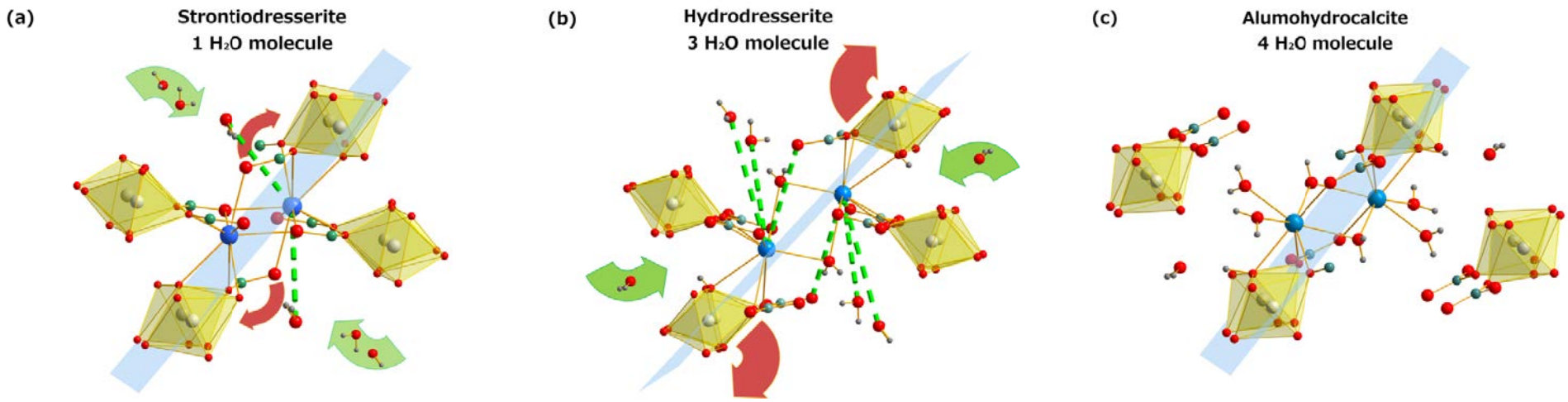

616 **Figure 11**. The surroundings of the M^{2+} site and their modification related to the number of water molecules. (a) Sr/Ca atom site environment
617 strintiochevkinite; (b) Ba^{2+} atom environment in dresserite; (c) Ca^{2+} atom environment in alumohydrocalcite. The light blue plane shows the Al – M^{2+} – M^{2}
618 Al coordination spheres interactions present in all structures from the group. Green arrows point where additional water would locate and red arrows show h
619 particular octahedra would reorganise to obtain the packing of the next, more hydrated mineral. Green dashed lines show the path of bond formation in n
620 structure.

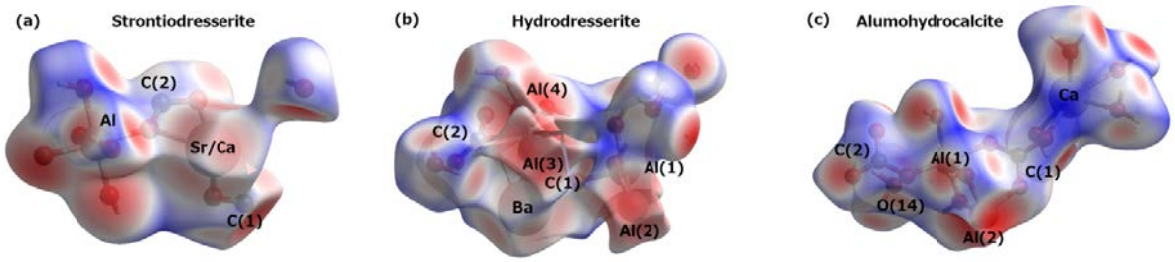

621

622 **Figure 12**. Projestion of the Hirshfeld surface (McKinnon, et al. 2007) around assymetric unit of (a)
623 strontiodresserite; (b) hydrodresserite; (c) alumohydrocalcite. The colour scale on the surface
624 represents the shortest distances from the surface coordinate to the closest atom outside or inside the
625 surface. Red corresponds to the shortest contacts(-0.90(5) Å), blue to the longest (1.05(4) Å).

626

627

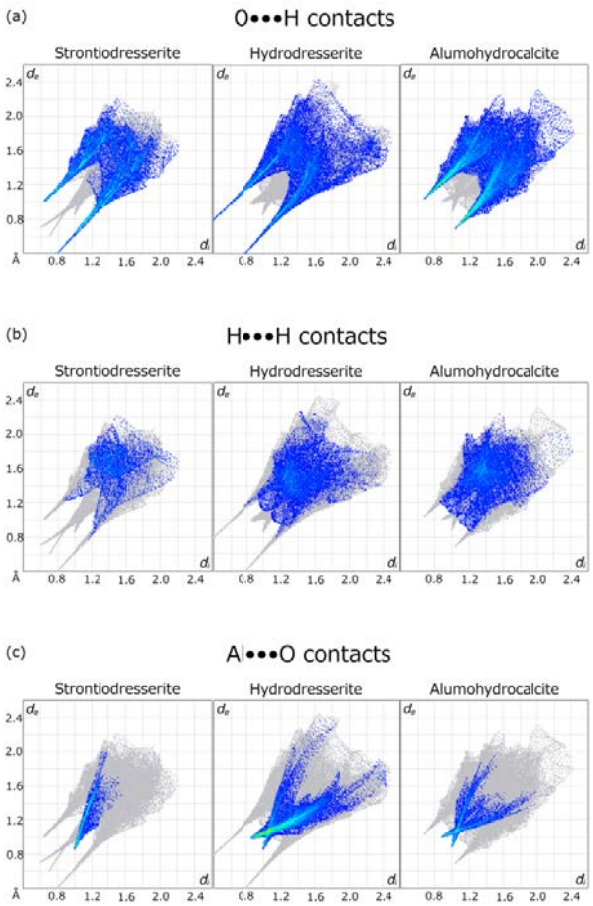

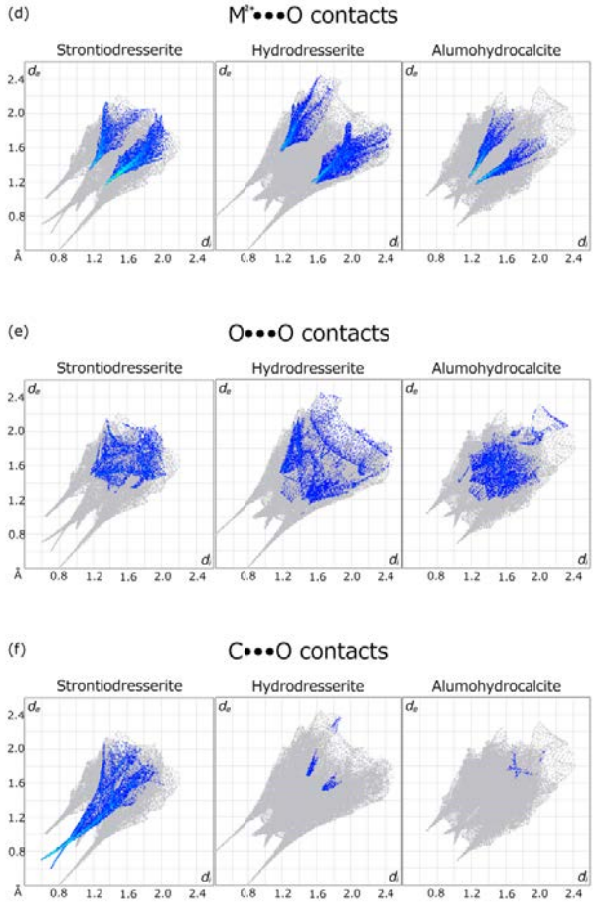

628 **Figure 13.** Comparison of fingerprint plots for the members with known crystal structure of the
629 dundasite group of minerals. Because dundasite does not have hydrogen atoms found in its crystal
630 structure, it was not taken for this comparison.
631

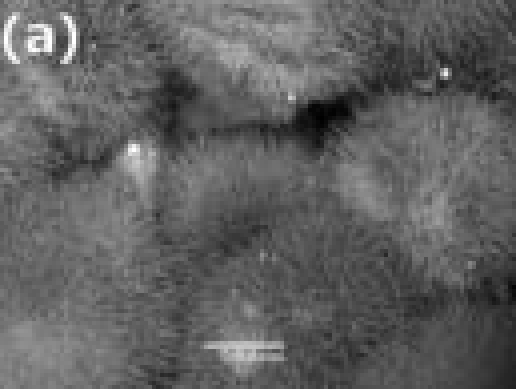
(a)

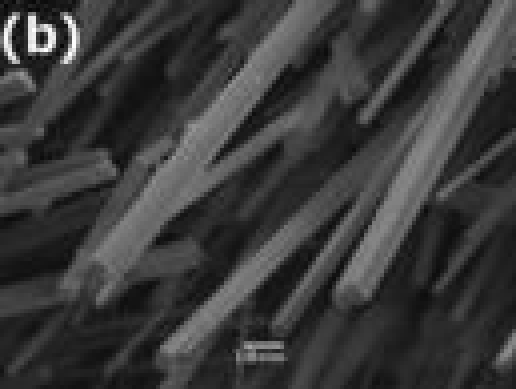
(b)

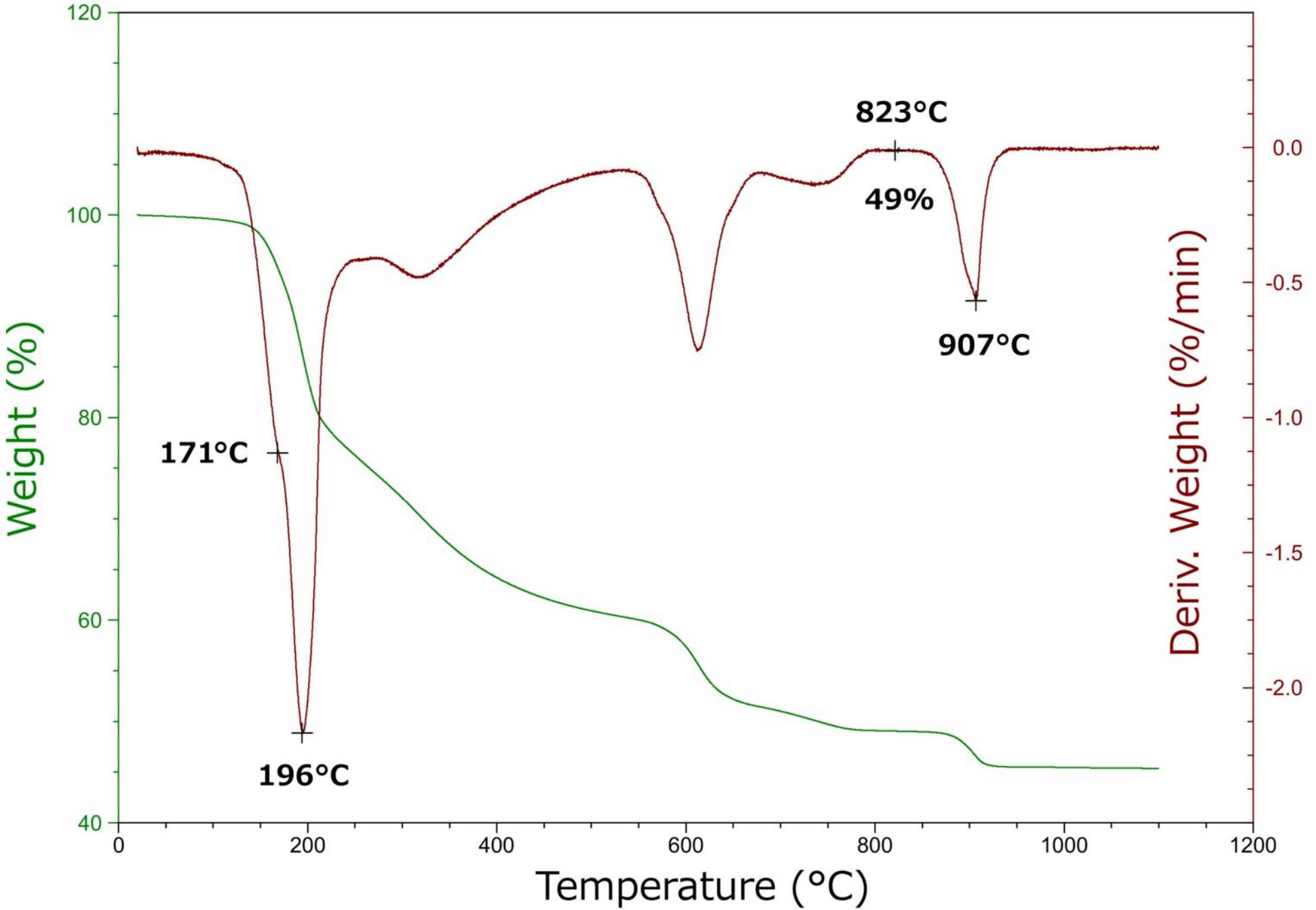
823°C
49%
907°C
171°C
196°C
Weight (%)
Deriv. Weight (%/min)
Temperature (°C)
120
100
80
60
40
0
200
400
600
800
1000
1200
0.0
-0.5
-1.0
-1.5
-2.0

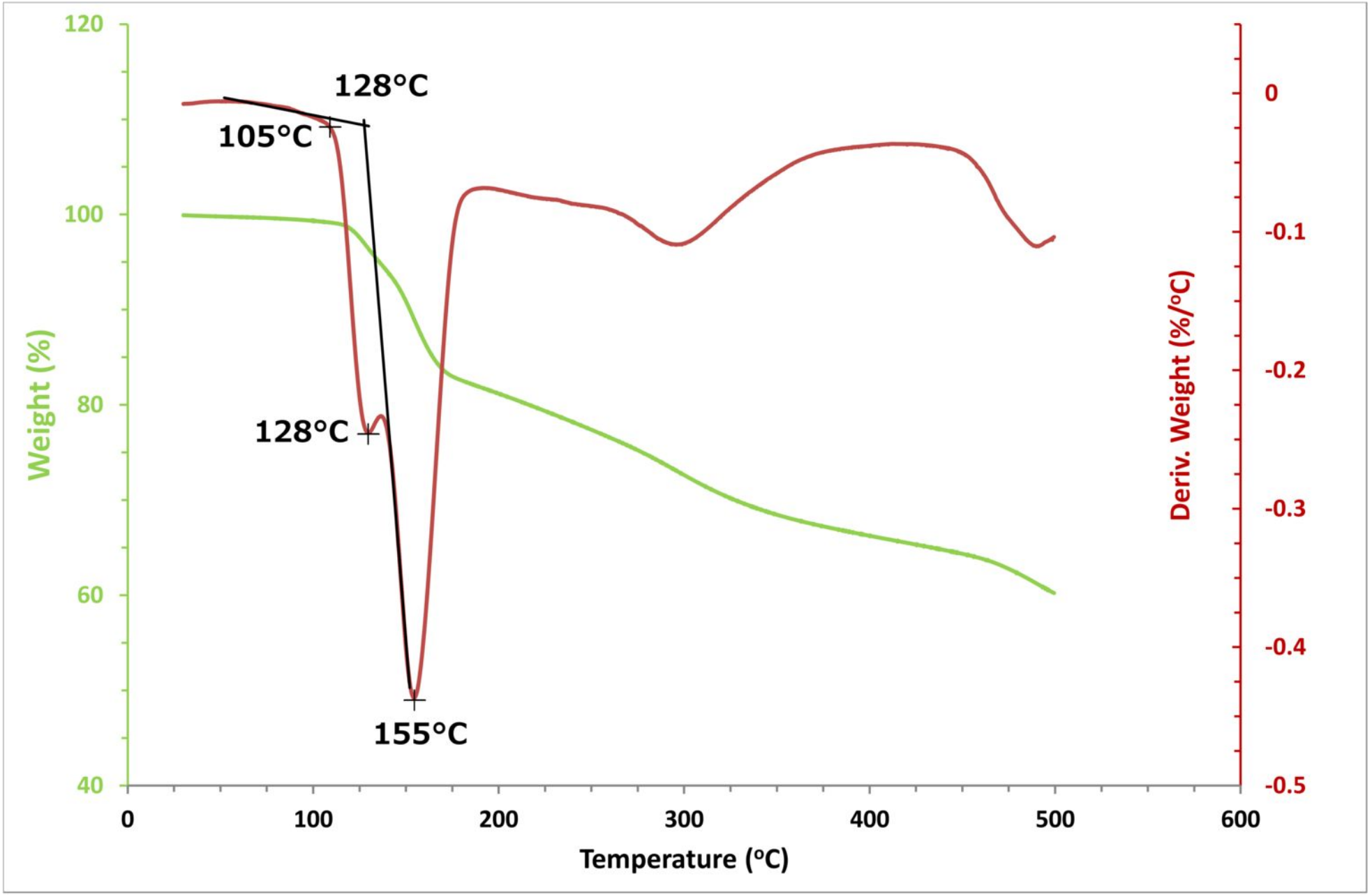
120
100
80
60
40
Weight (%)
128°C
105°C
128°C
155°C
0
-0.1
-0.2
-0.3
-0.4
-0.5
Deriv. Weight (%/°C)
0
100
200
300
400
500
600
Temperature (°C)

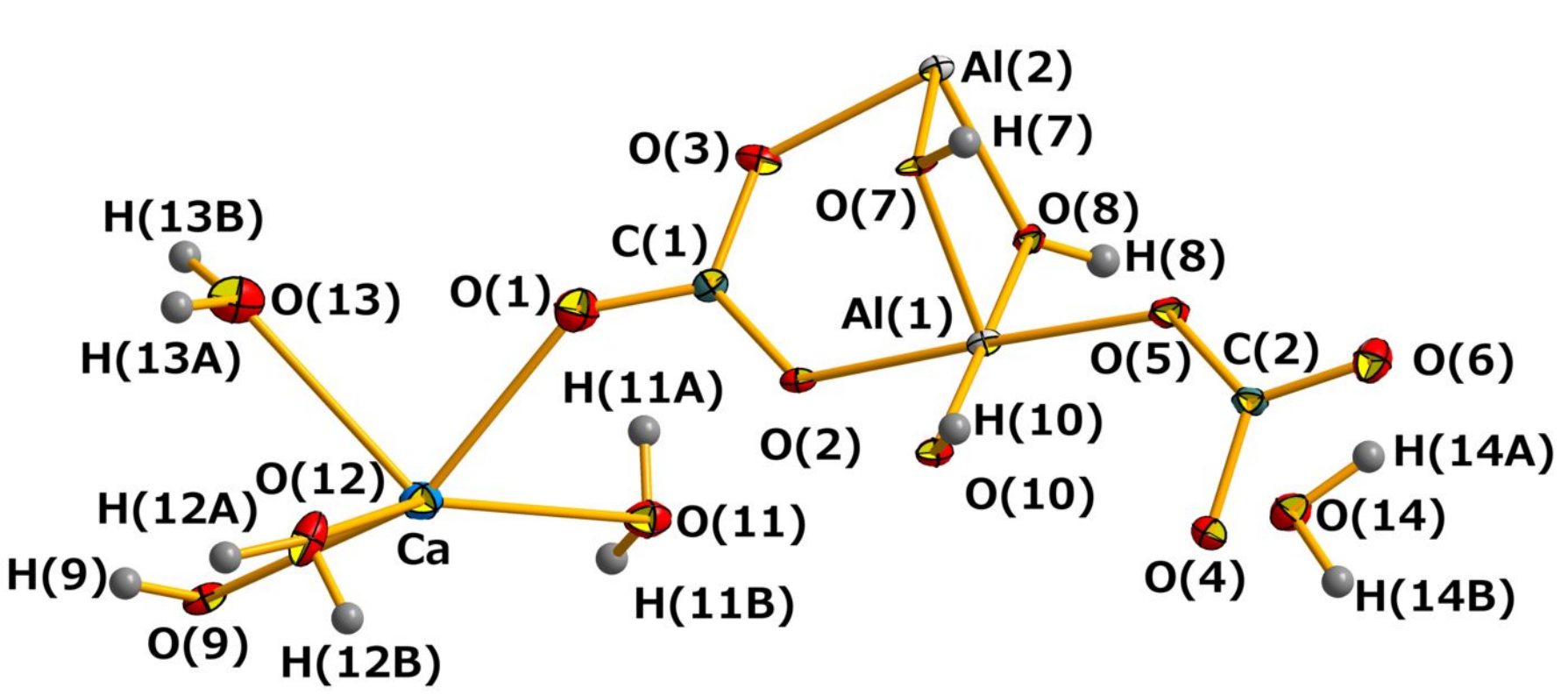
Al(2)
H(7)
O(3)
O(7)
O(8)
H(8)
H(13B)
C(1)
O(13)
O(1)
Al(1)
O(5)
C(2)
O(6)
H(13A)
H(11A)
O(2)
H(10)
O(10)
H(14A)
O(12)
H(12A)
O(11)
O(14)
Ca
O(4)
H(9)
H(11B)
H(14B)
O(9)
H(12B)

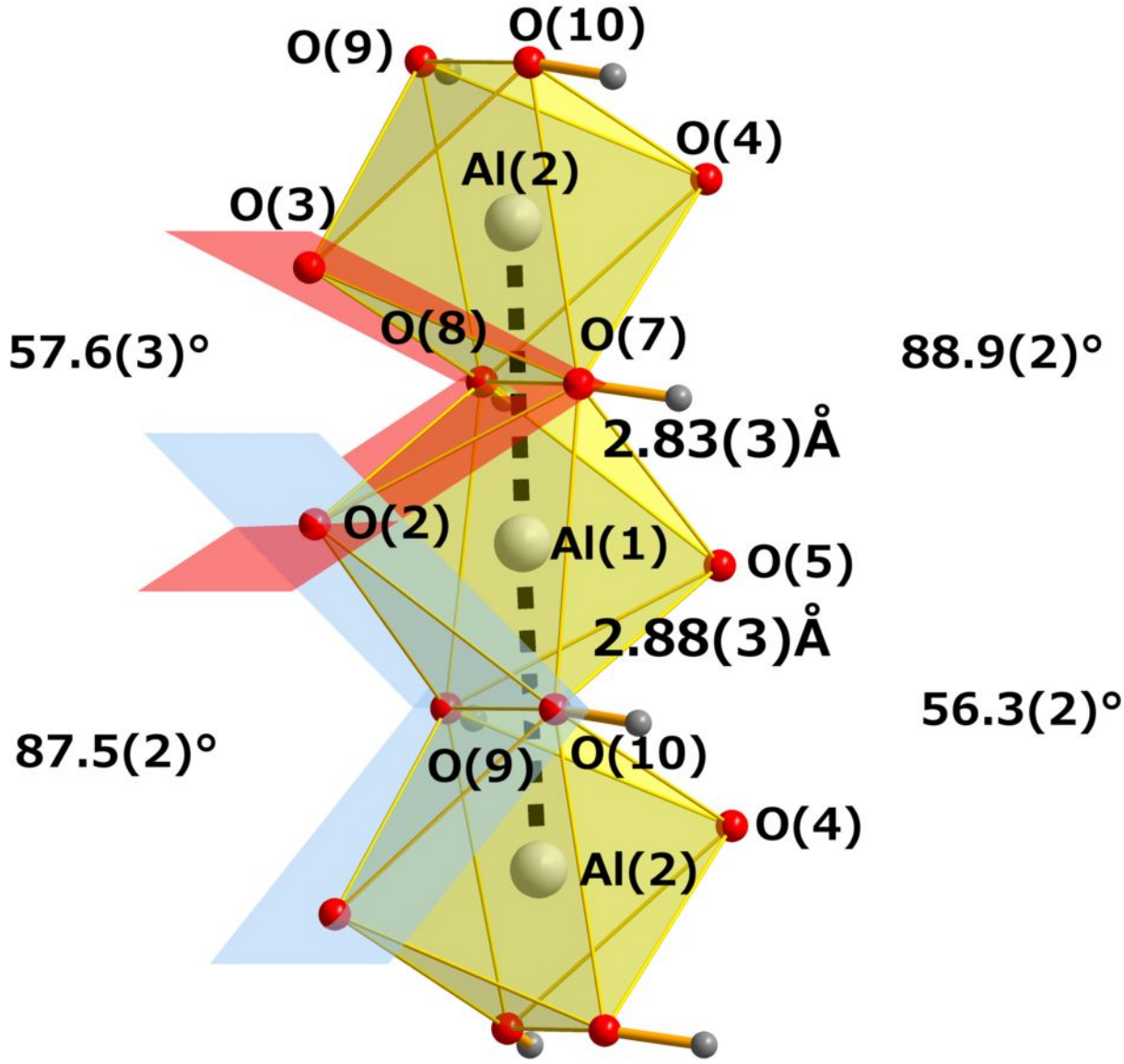
O(9)
O(10)
O(4)
Al(2)
O(3)
57.6(3)°
O(8)
O(7)
88.9(2)°
2.83(3)Å
O(2)
Al(1)
O(5)
2.88(3)Å
56.3(2)°
87.5(2)°
O(9)
O(10)
O(4)
Al(2)

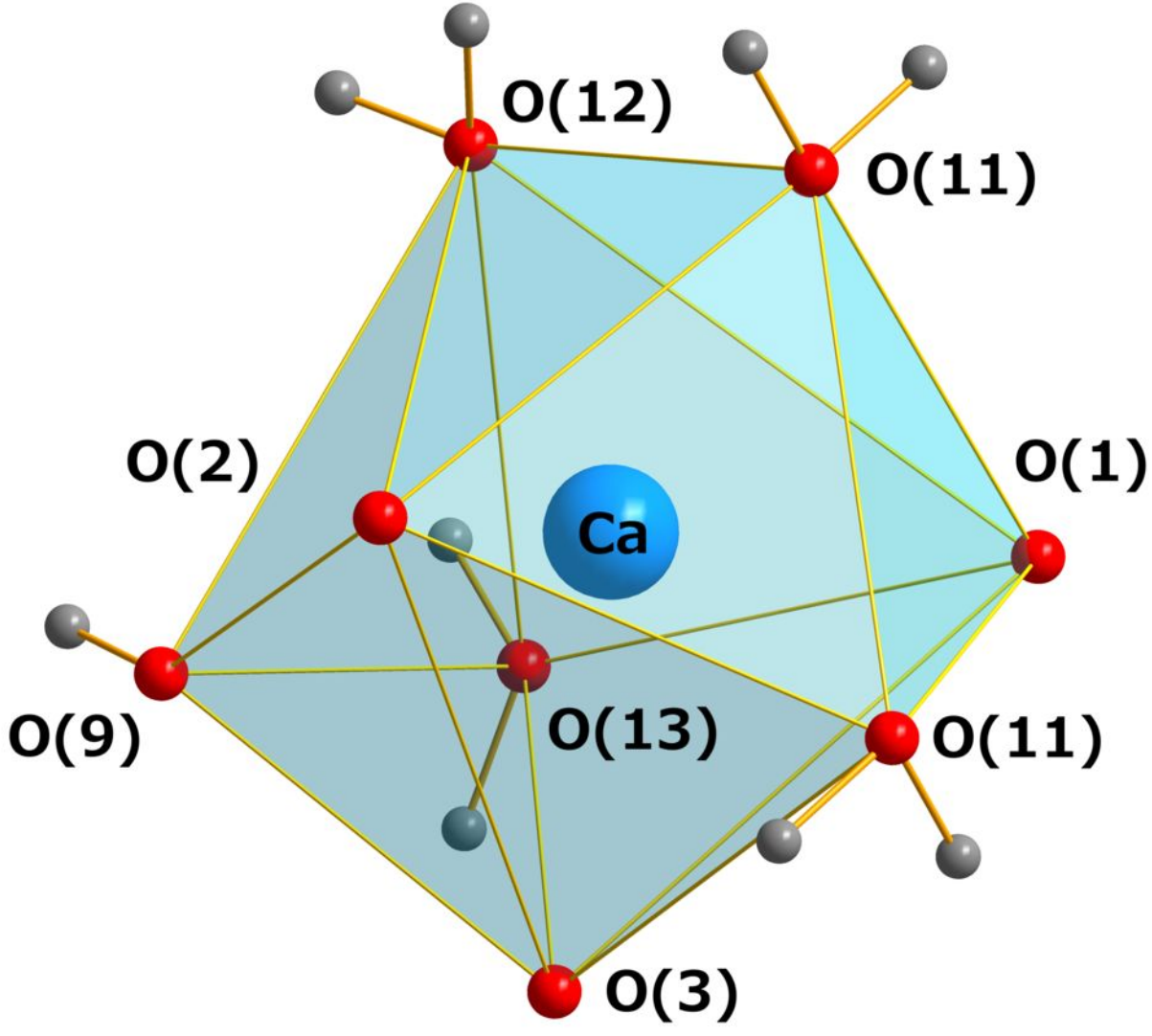
O(12)
O(11)
O(2)
O(1)
Ca
O(9)
O(13)
O(11)
O(3)

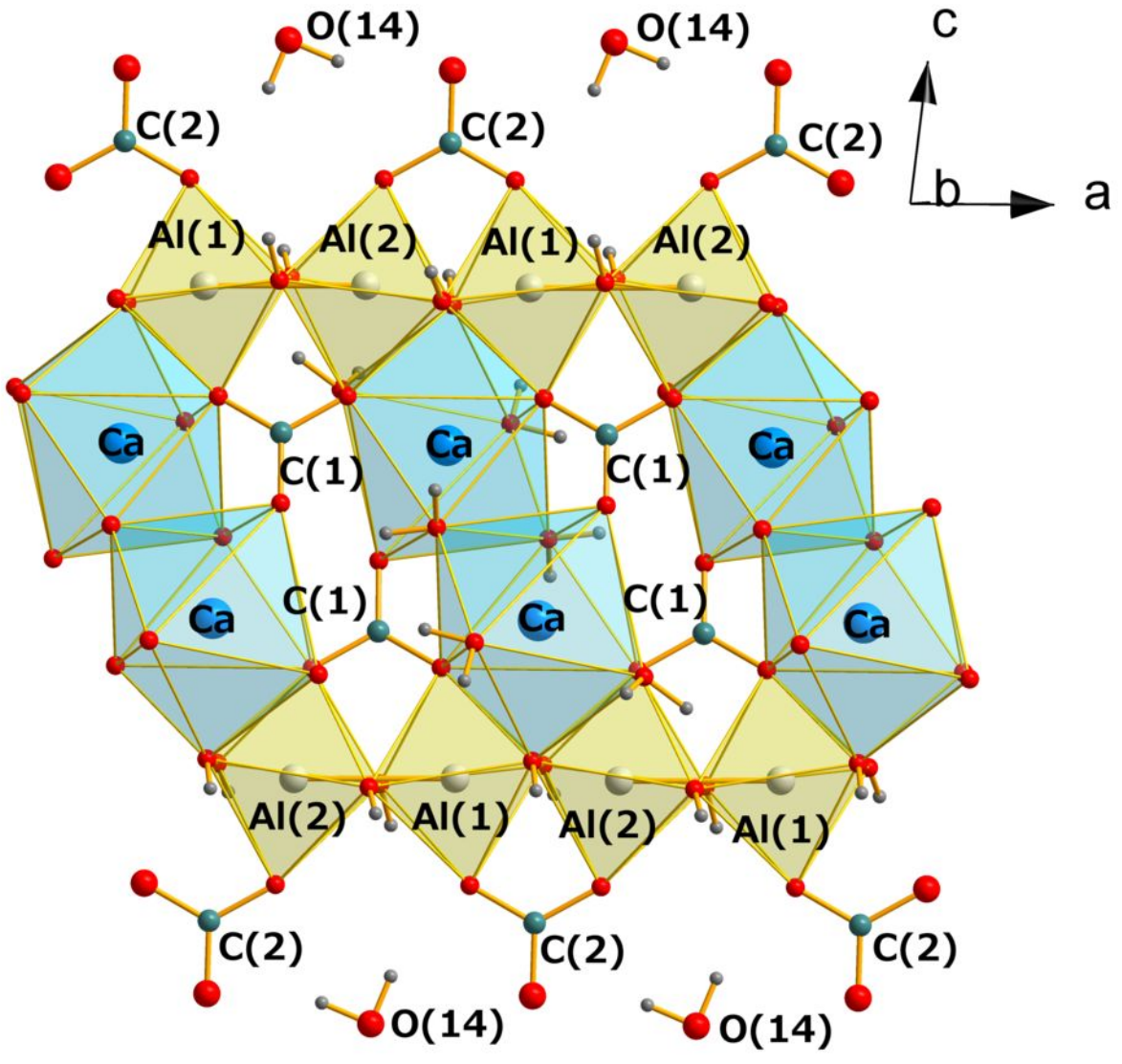
O(14)
O(14)
c
C(2)
C(2)
C(2)
b
a
Al(1)
Al(2)
Al(1)
Al(2)
Ca
Ca
Ca
C(1)
C(1)
C(1)
C(1)
Ca
Ca
Ca
Al(2)
Al(1)
Al(2)
Al(1)
C(2)
C(2)
C(2)
O(14)
O(14)

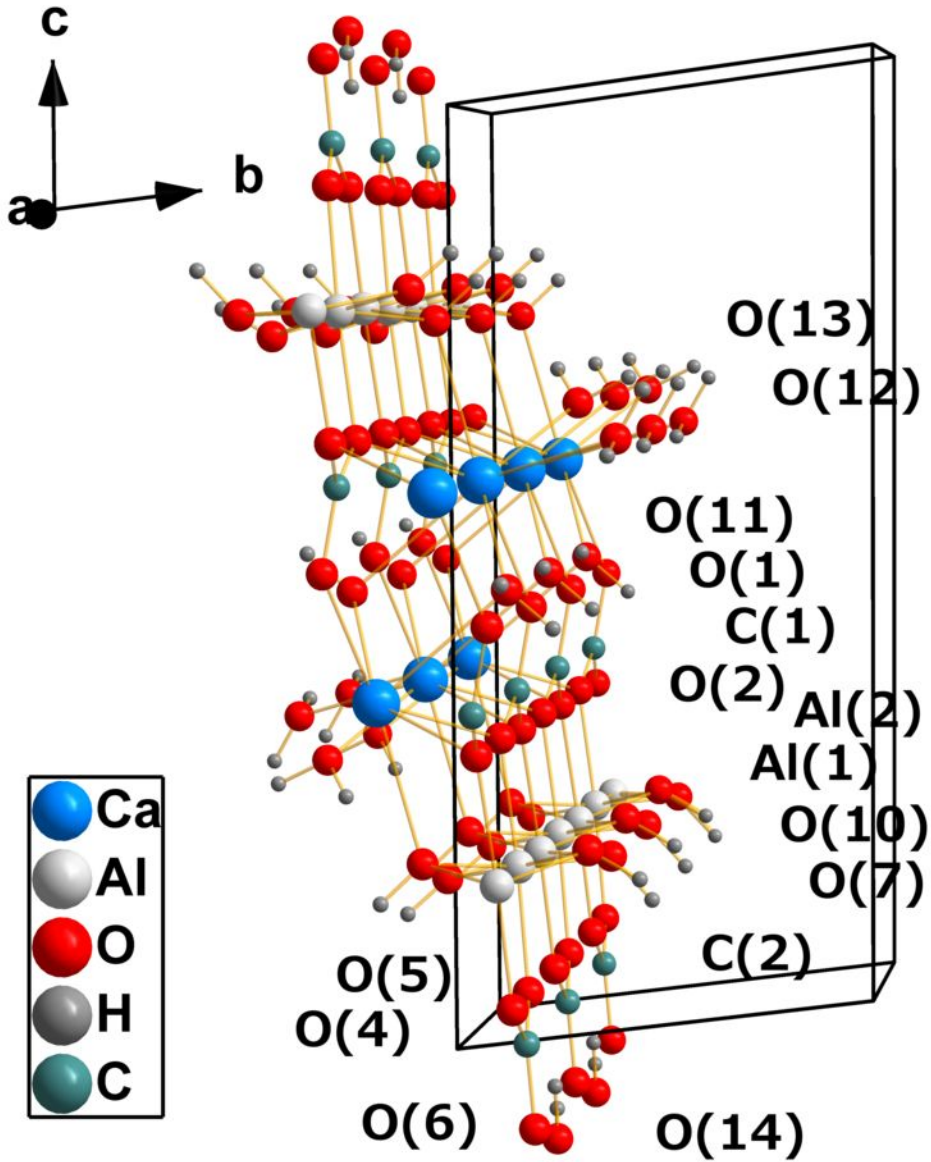
c
b
a
O(13)
O(12)
O(11)
O(1)
C(1)
O(2)
Al(2)
Al(1)
O(10)
O(7)
C(2)
O(5)
O(4)
O(6)
O(14)
Ca
Al
O
H
C

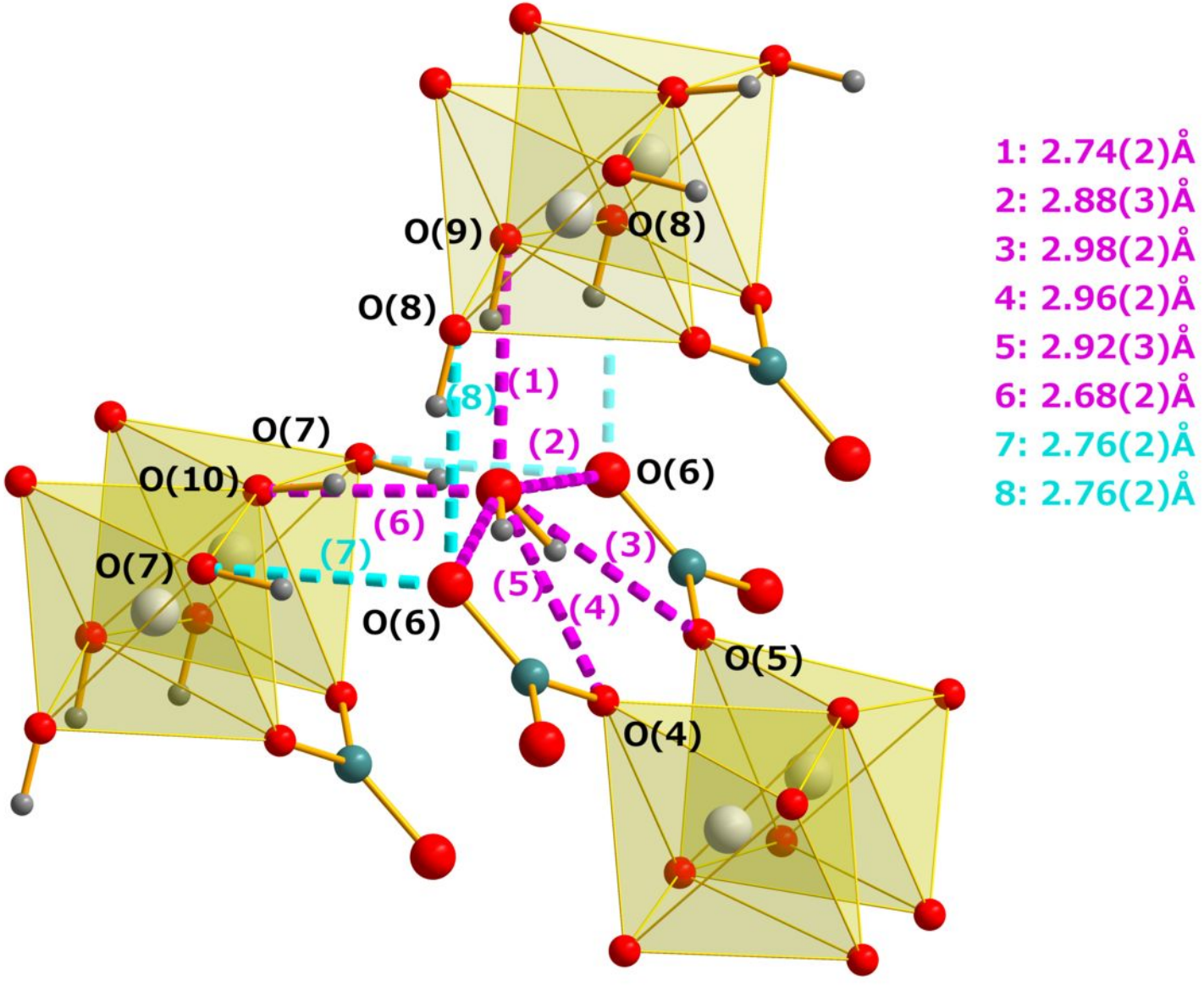
O(9)
O(8)
O(8)
(8)
(1)
O(7)
(2)
O(6)
O(10)
(6)
(3)
O(7)
(7)
(5)
(4)
O(6)
O(5)
O(4)
1: 2.74(2)Å
2: 2.88(3)Å
3: 2.98(2)Å
4: 2.96(2)Å
5: 2.92(3)Å
6: 2.68(2)Å
7: 2.76(2)Å
8: 2.76(2)Å

(a) Dundasite, strontiodresserite

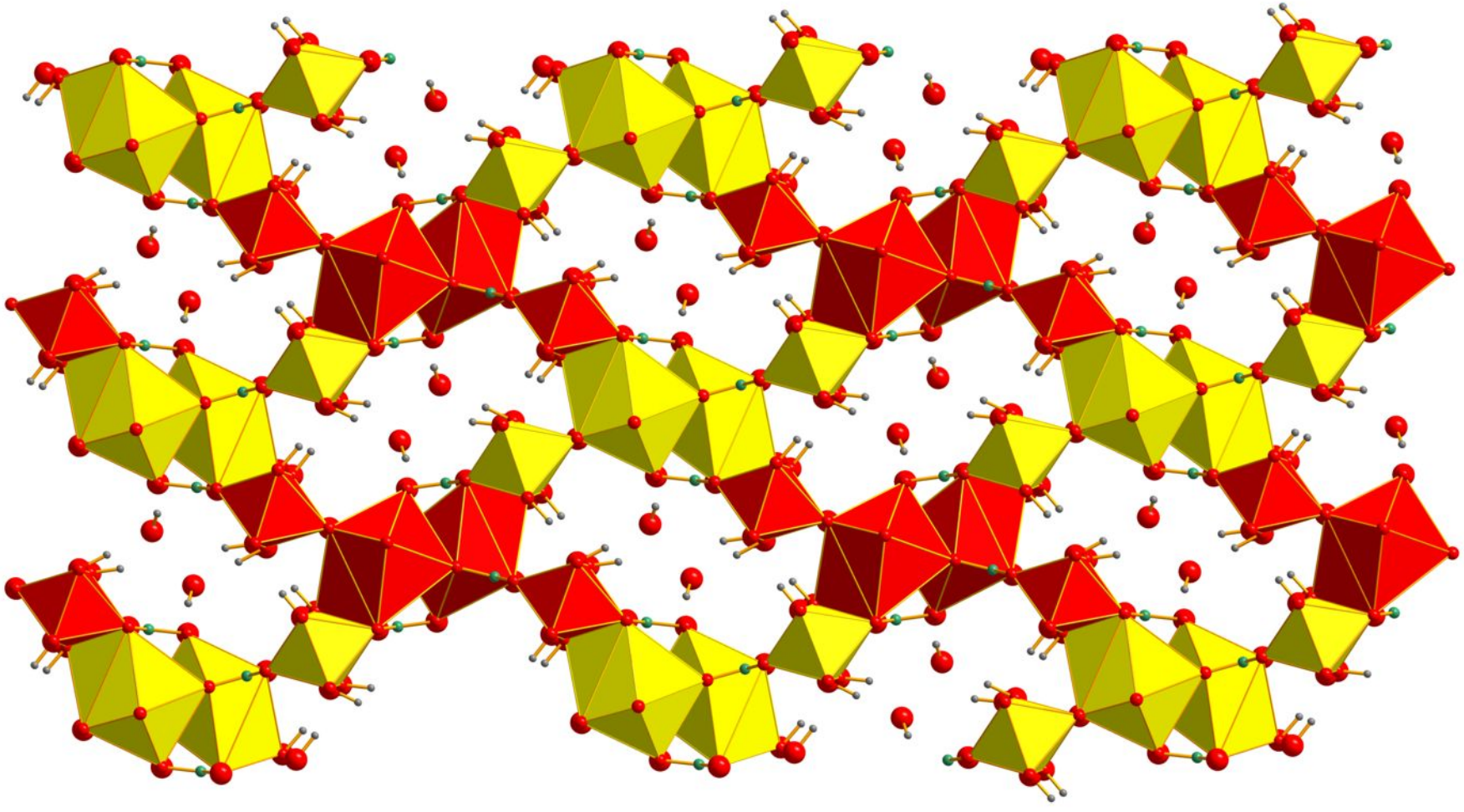

(b)

Hydrodresserite

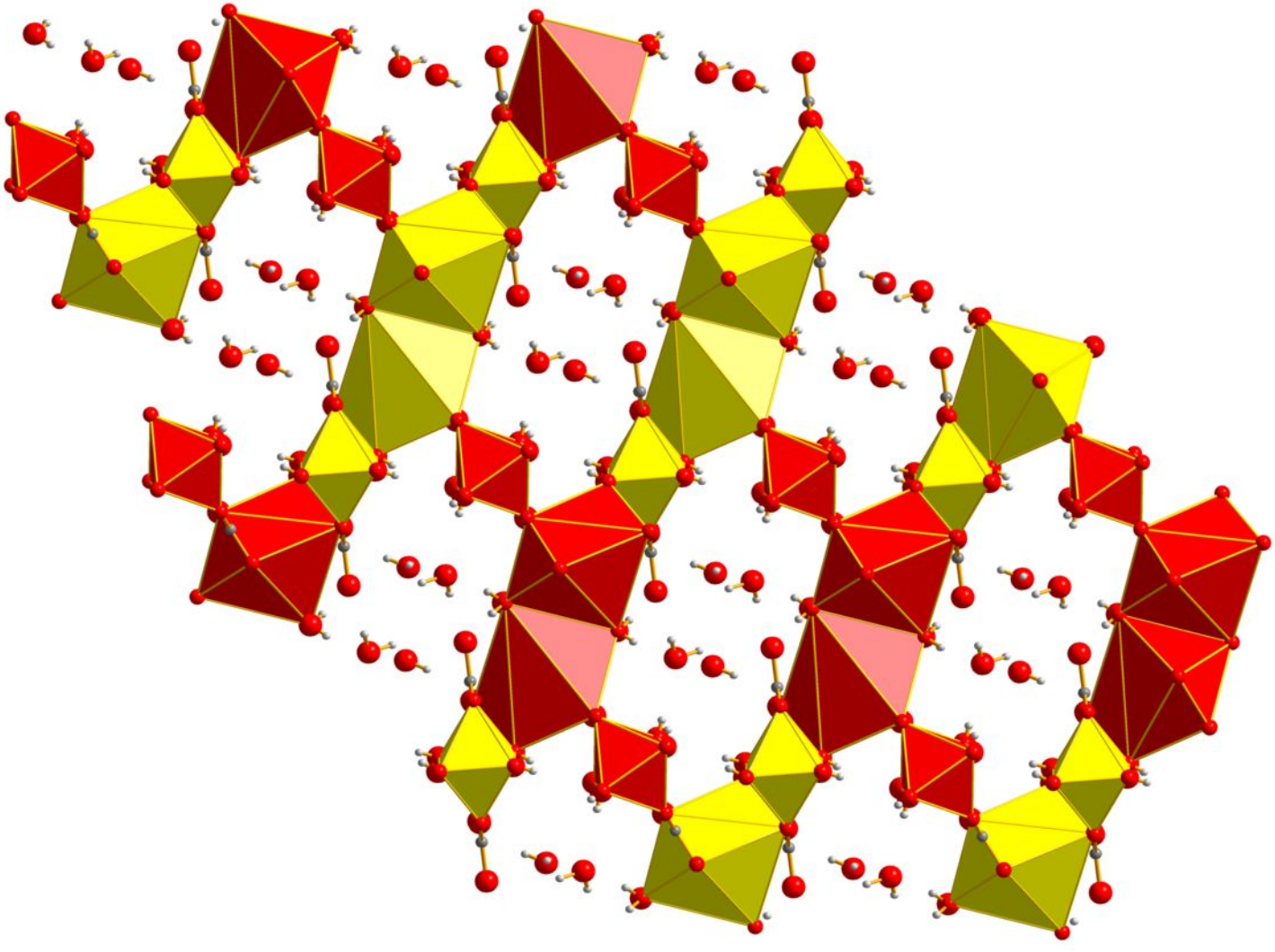

(c) Alumohydrocalcite

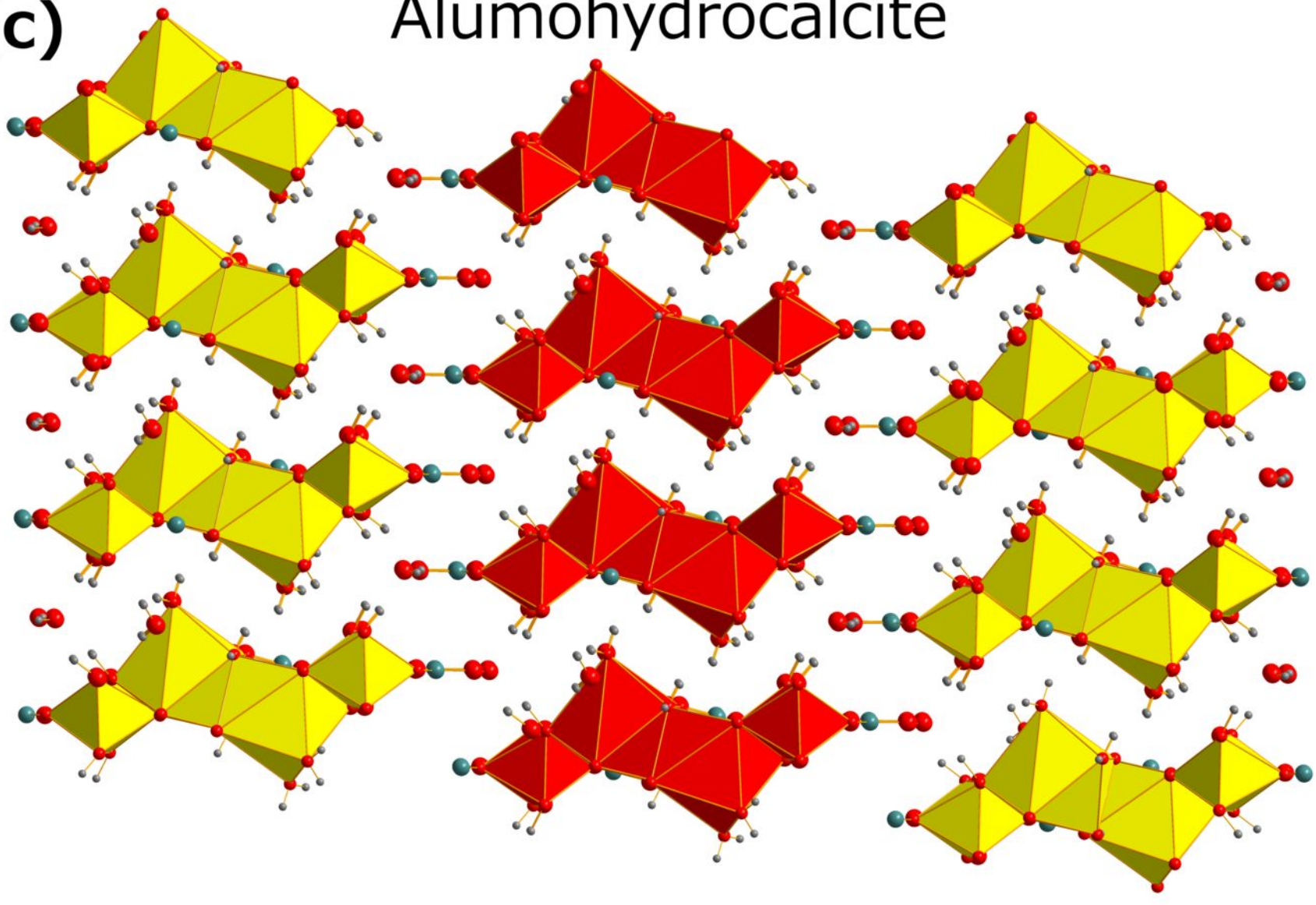

(a)

Strontiodresserite

1 H_2O molecule

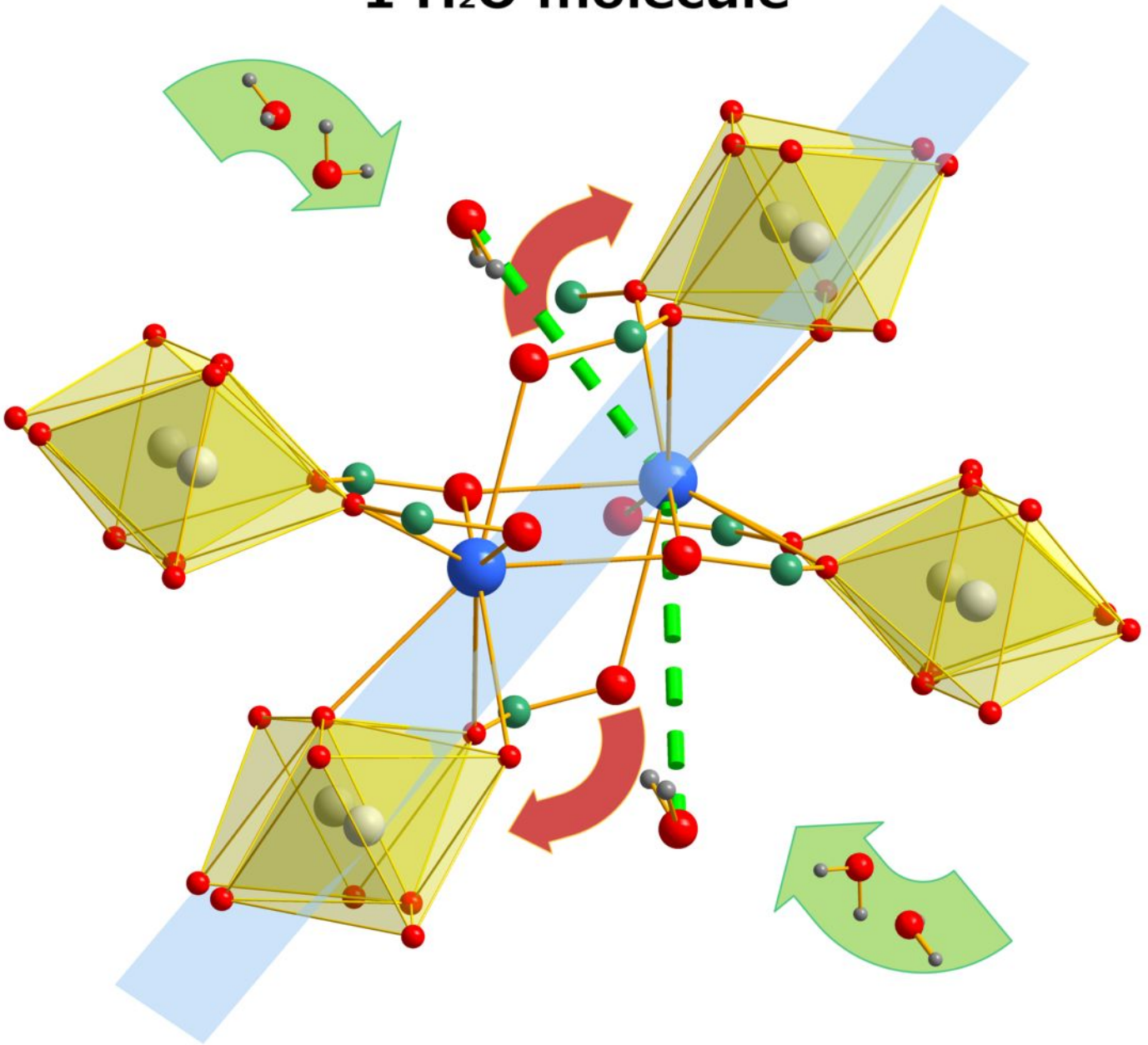

(b)

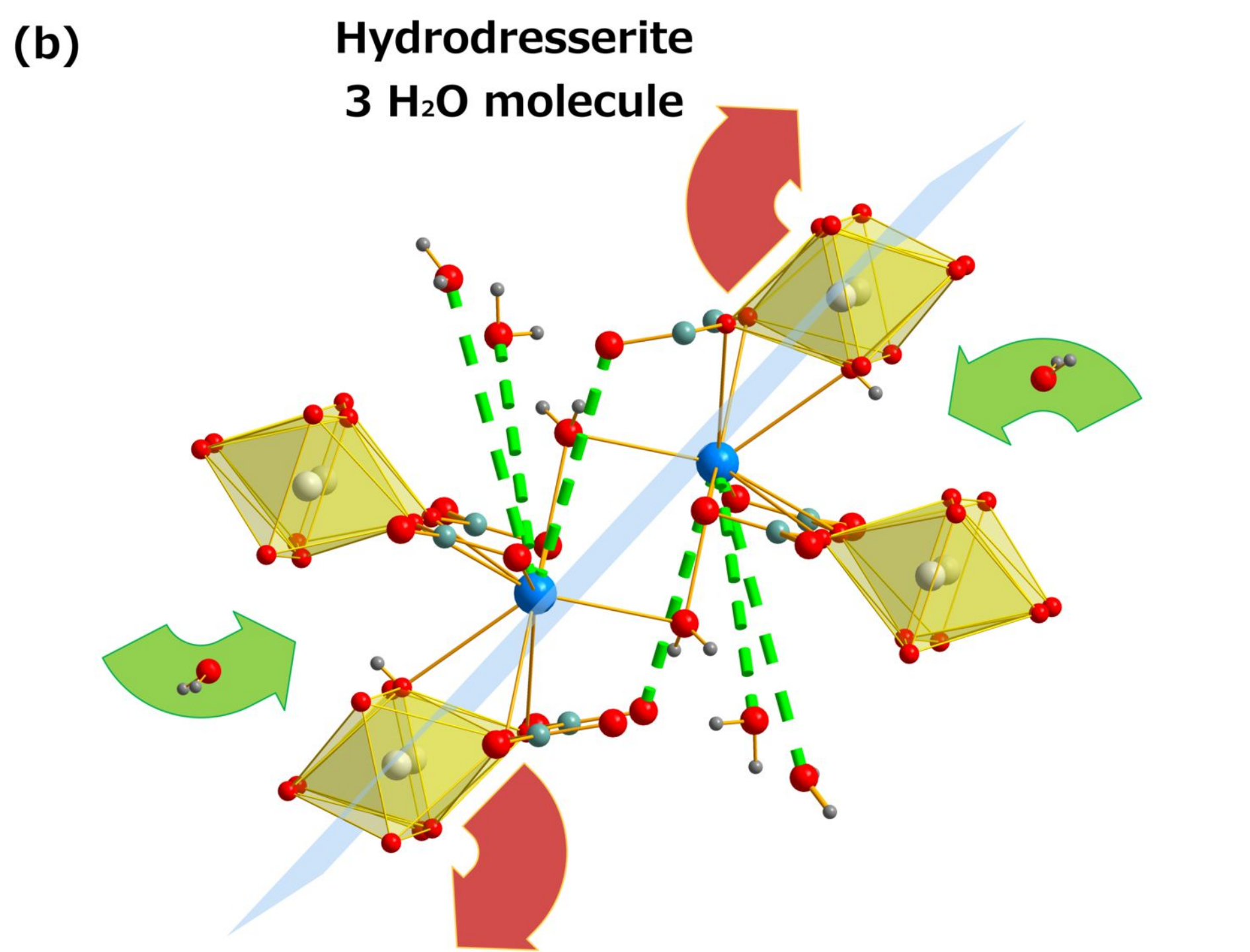

(c)

Alumohydrocalcite

4 H_2O molecule

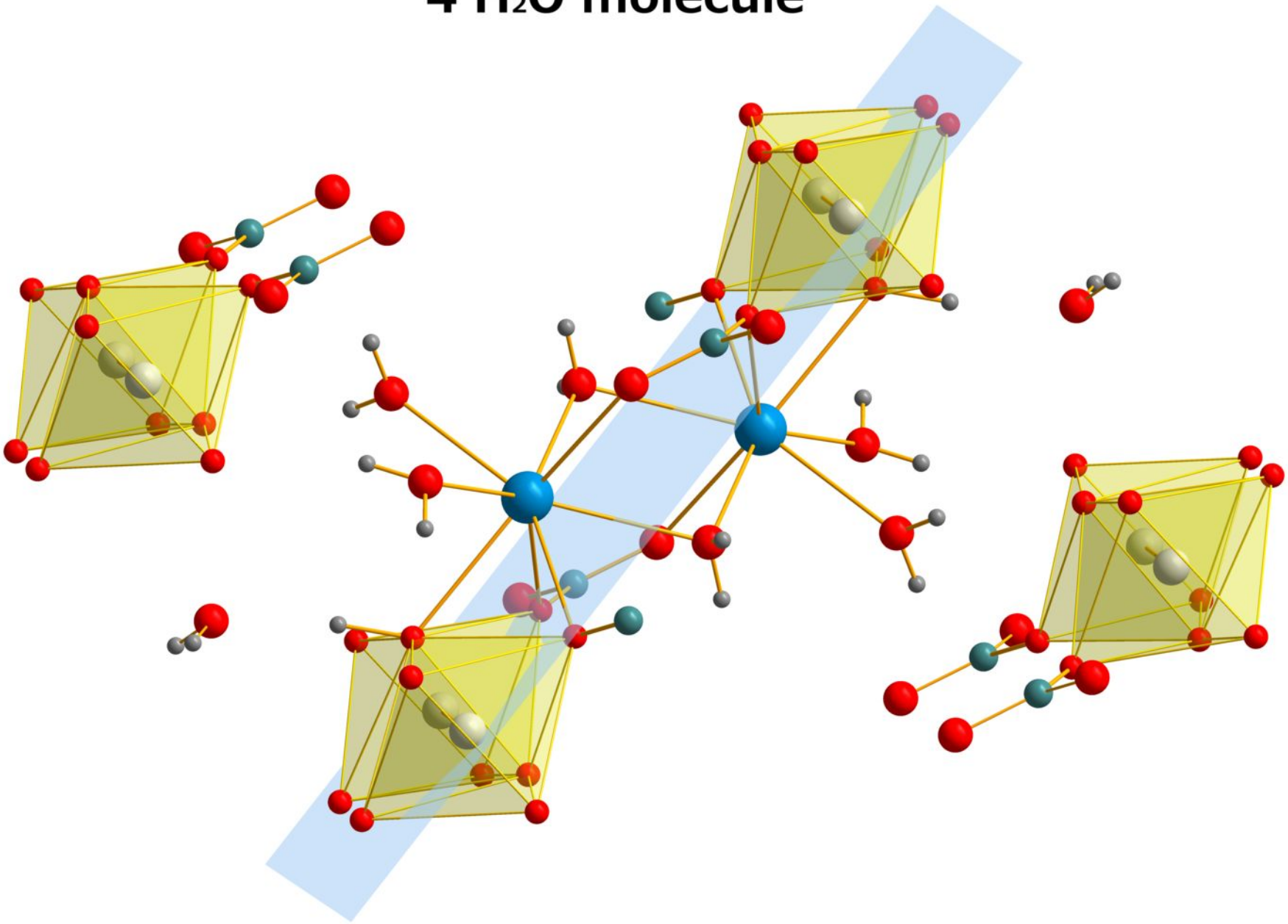

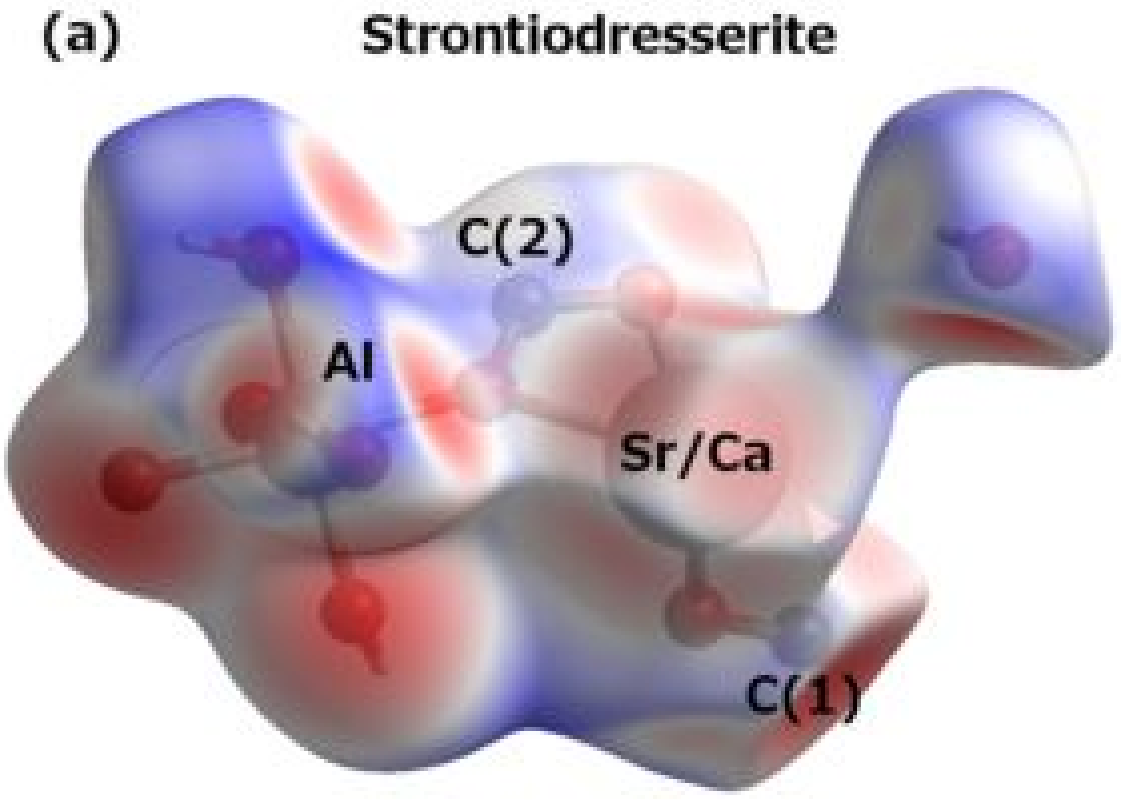
(a)
Strontiodresserite
C(2)
Al
Sr/Ca
C(1)

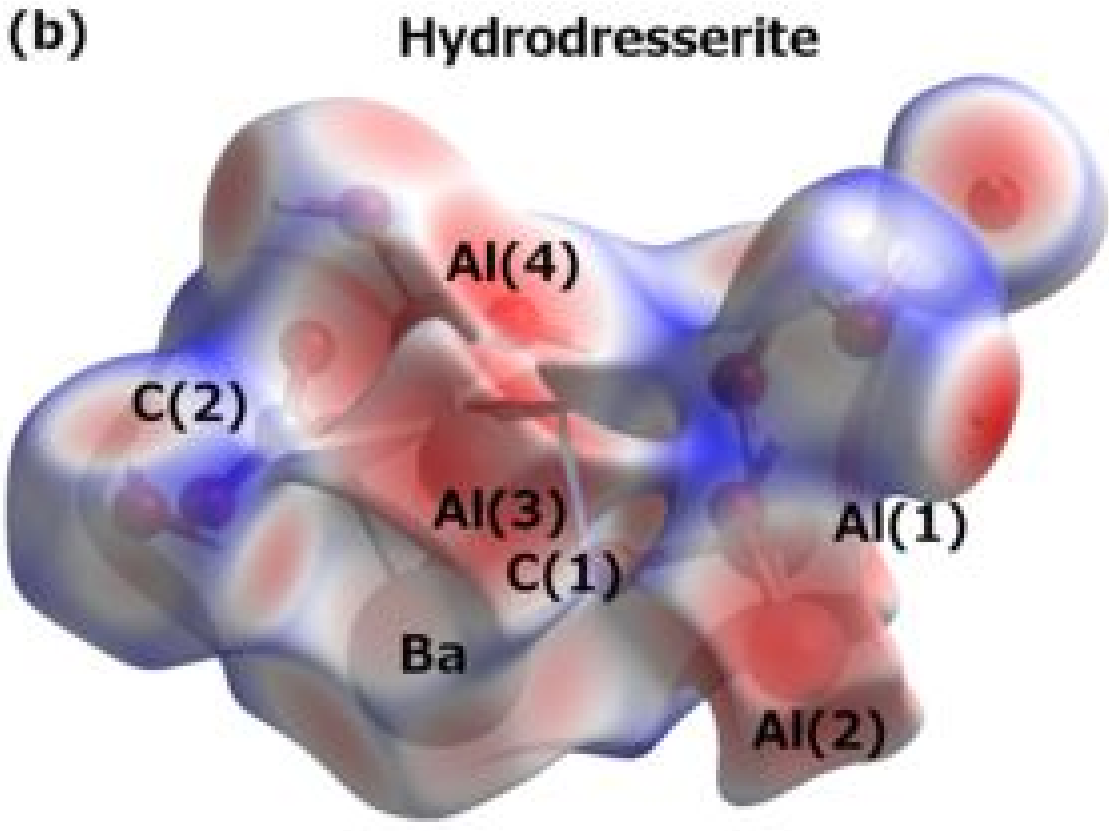
(b)
Hydrodresserite
Al(4)
C(2)
Al(3)
C(1)
Ba
Al(1)
Al(2)

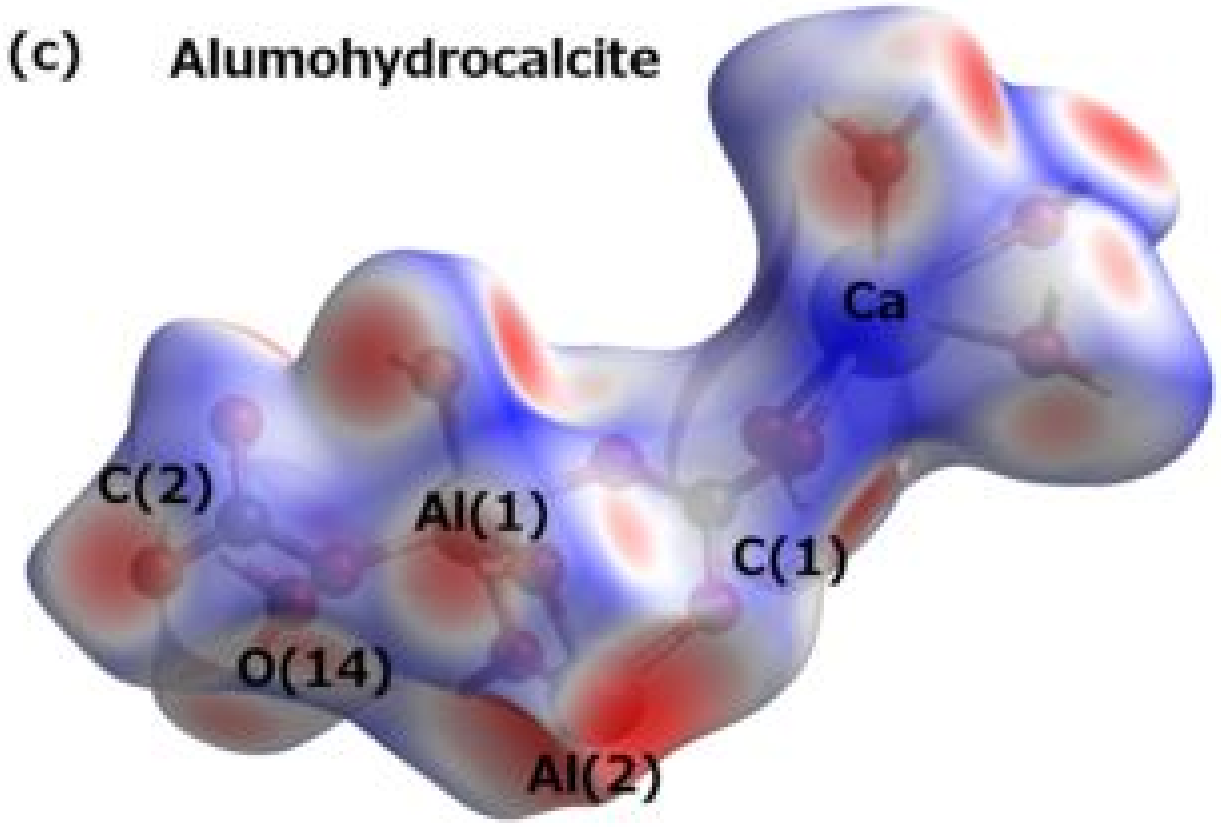
(c) Alumohydrocalcite
Ca
C(2)
Al(1)
C(1)
O(14)
Al(2)

(a)

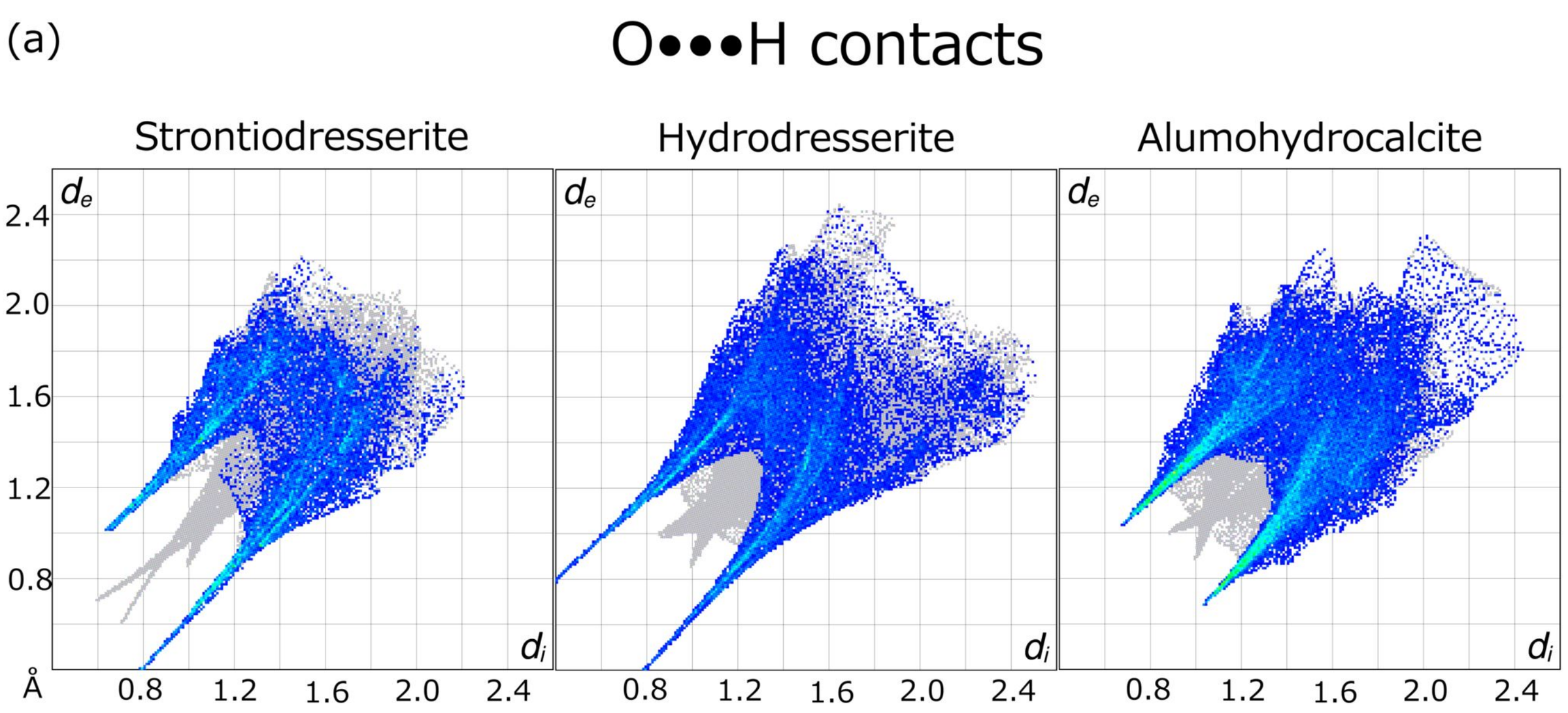
O•••H contacts
Strontiodresserite
Hydrodresserite
Alumohydrocalcite
d_e
d_i
2.4
2.0
1.6
1.2
0.8
Å
0.8
1.2
1.6
2.0
2.4

(b)

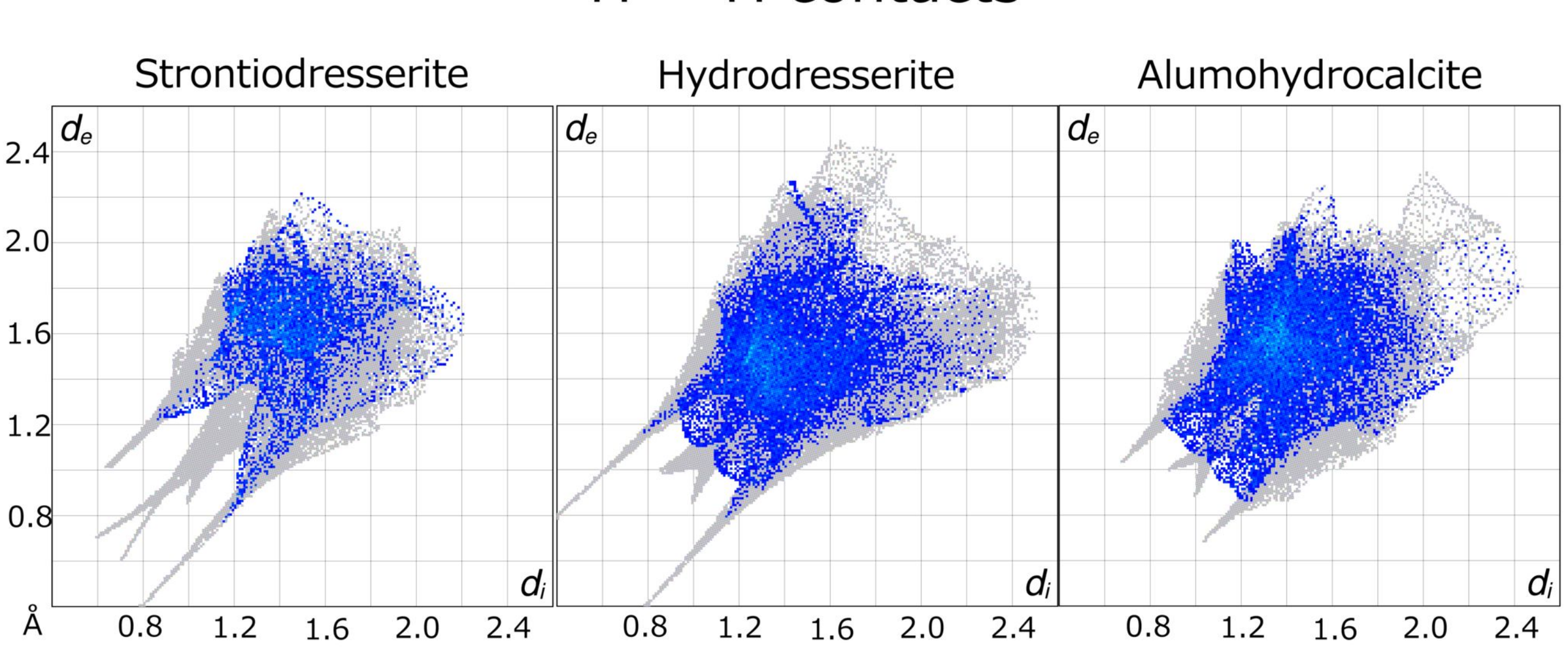
H•••H contacts
Strontiodresserite
Hydrodresserite
Alumohydrocalcite
d_e
d_i
2.4
2.0
1.6
1.2
0.8
Å
0.8
1.2
1.6
2.0
2.4

(c)

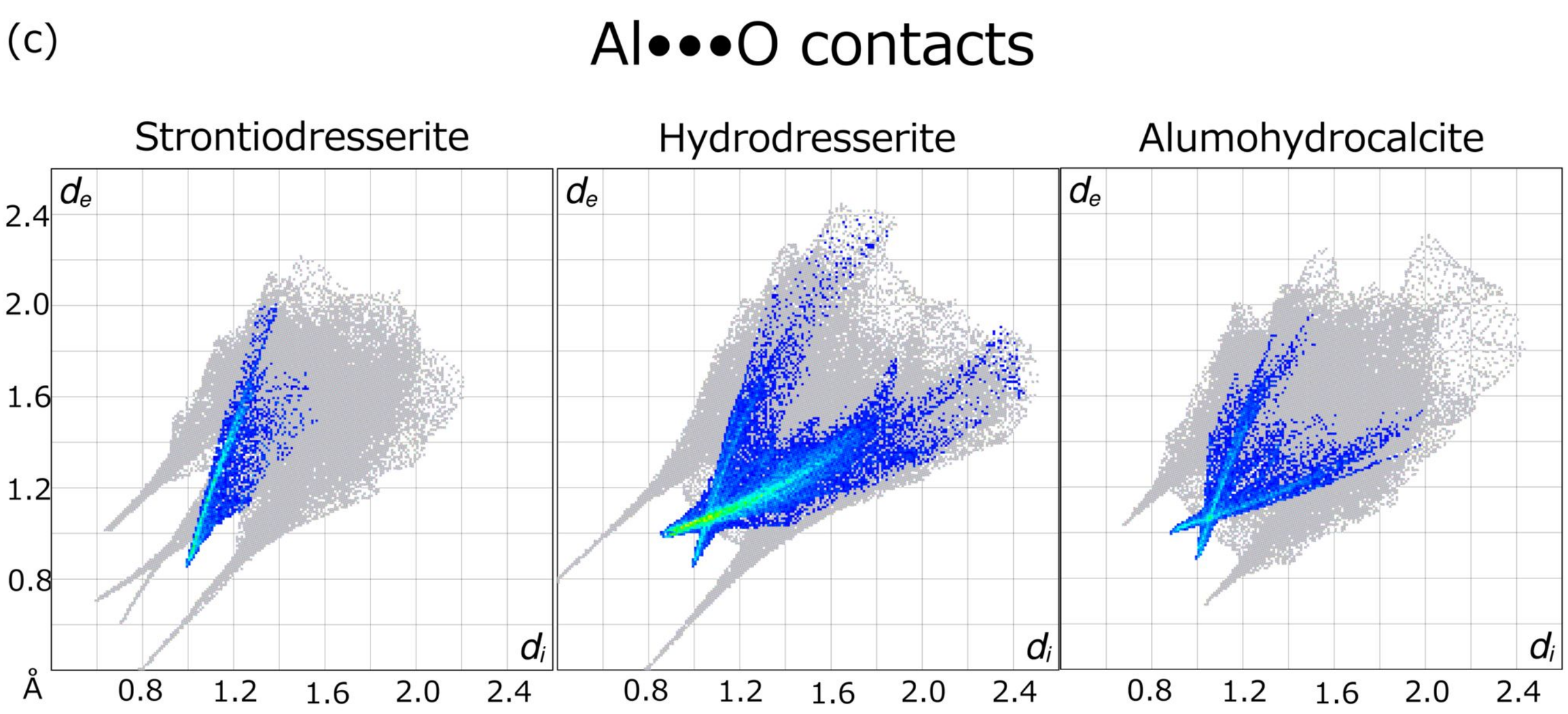
Al•••O contacts
Strontiodresserite
Hydrodresserite
Alumohydrocalcite
d_e
d_i
2.4
2.0
1.6
1.2
0.8
Å
0.8
1.2
1.6
2.0
2.4

(d)

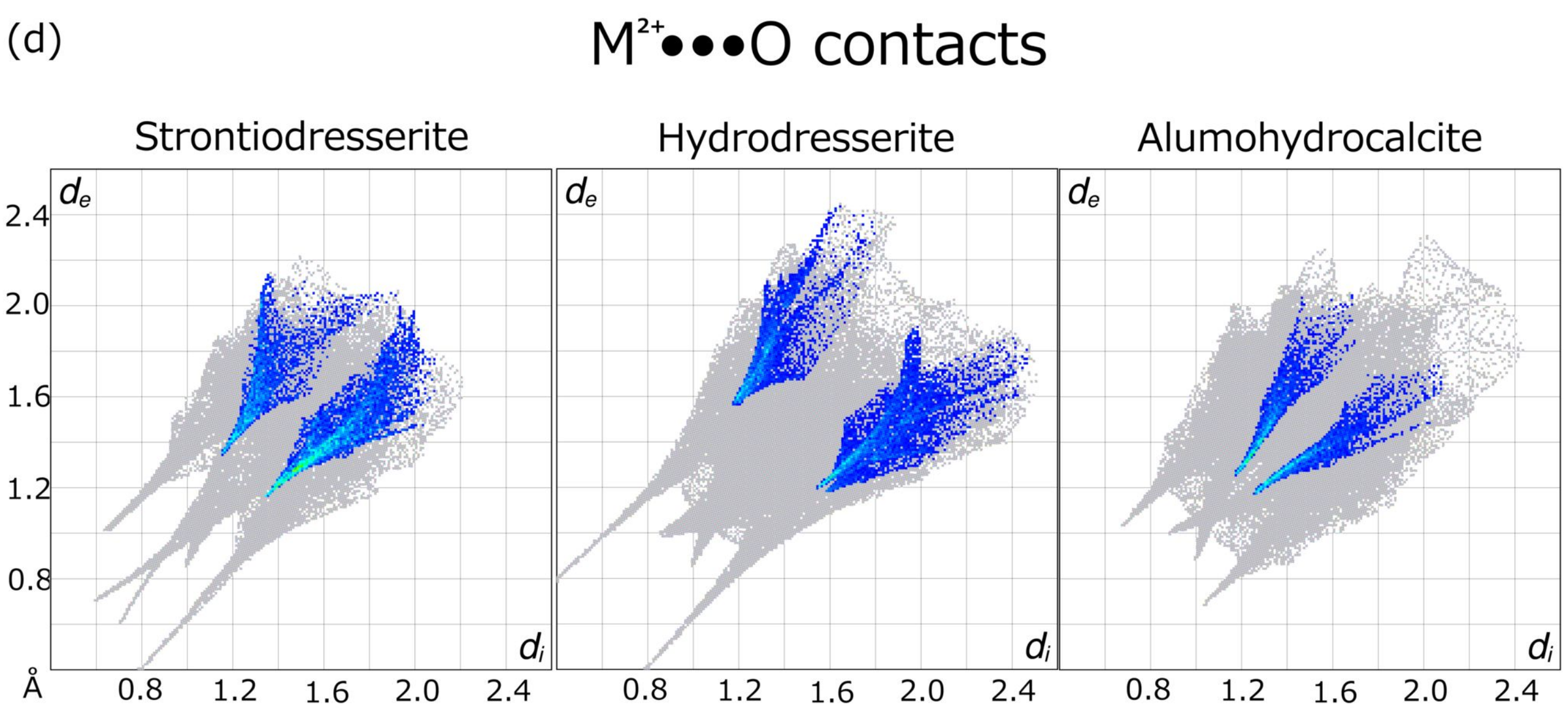
M2+•••O contacts
Strontiodresserite
Hydrodresserite
Alumohydrocalcite
de
di
2.4
2.0
1.6
1.2
0.8
Å
0.8
1.2
1.6
2.0
2.4

(e)

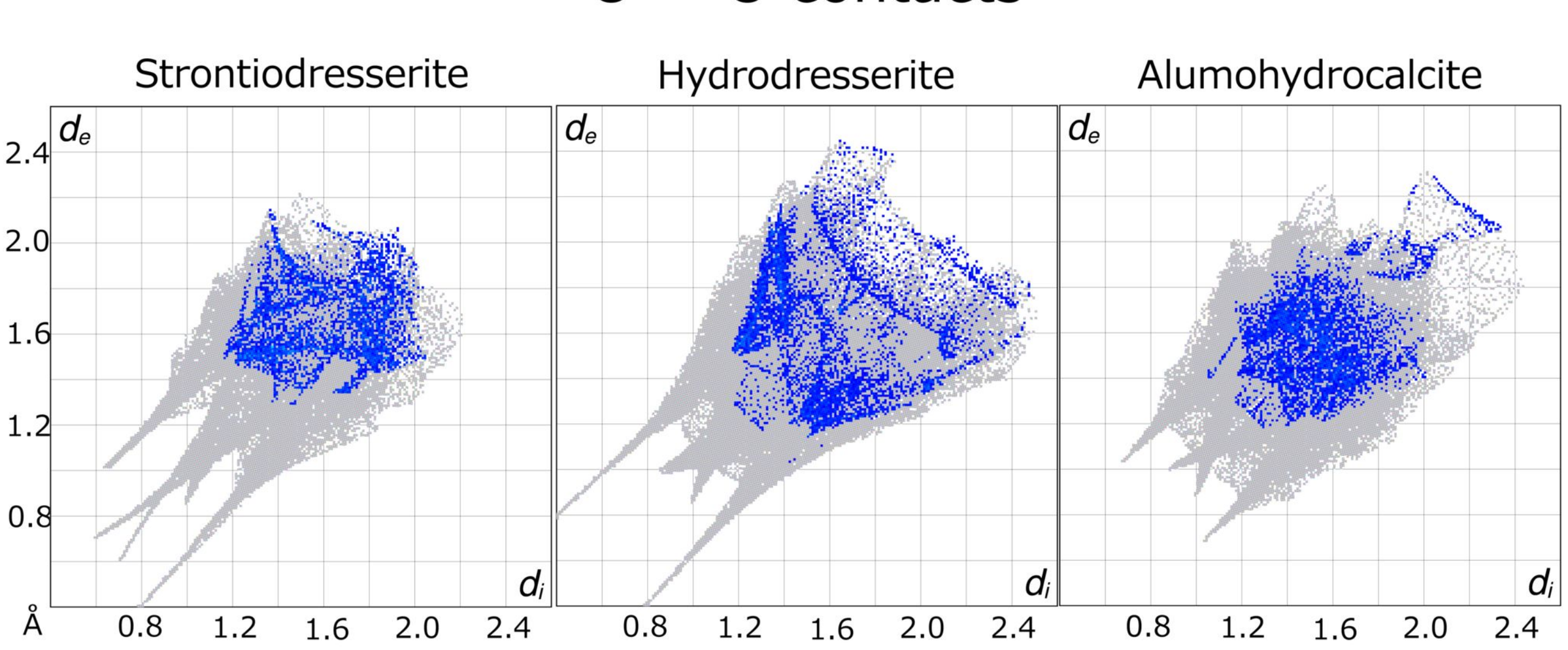
O•••O contacts
Strontiodresserite
Hydrodresserite
Alumohydrocalcite
d_e
d_i
2.4
2.0
1.6
1.2
0.8
Å
0.8
1.2
1.6
2.0
2.4

(f)

C•••O contacts